MIRROR SYMMETRY, LAURENT INVERSION AND THE CLASSIFICATION OF $\mathbb{Q}$-FANO THREEFOLDS

TOM COATES, LIANA HEUBERGER, AND ALEXANDER M. KASPRZYK

ABSTRACT. We describe recent progress in a program to understand the classification of three-dimensional Fano varieties with $\mathbb{Q}$-factorial terminal singularities using mirror symmetry. As part of this we give an improved and more conceptual understanding of Laurent inversion, a technique that sometimes allows one to construct a Fano variety X directly from a Laurent polynomial f that corresponds to it under mirror symmetry.

1. INTRODUCTION

$\mathbb{Q}$-Fano threefolds are three-dimensional Fano varieties with at worst $\mathbb{Q}$-factorial terminal singularities. They play an important role in the Minimal Model Program [9, 44, 55, 58, 59]. In this paper we consider the classification of $\mathbb{Q}$-Fano threefolds up to $\mathbb{Q}$-Gorenstein (qG) deformation. It is known that there are finitely many deformation families [56], and many such families have been constructed explicitly [14, 15, 19, 34, 37, 47, 50, 63–65, 67], but the classification is still far from understood. We will describe a new approach to the classification problem, which is motivated by mirror symmetry. This approach has been successful in recovering the (known) classifications of smooth Fano varieties in dimensions two and three [22, 23], and in classifying singular del Pezzo surfaces [1, 33, 53]. The key idea is that there should be a one-to-one correspondence between equivalence classes of Fano varieties with mild singularities and equivalence classes of certain Laurent polynomials. The equivalence relation on Fano varieties here is qG-deformation; the equivalence relation on Laurent polynomials is mutation [2].

Definition 1. A Fano variety is of *class TG* (for 'toric generisation') if it occurs as the general fiber of a qG-degeneration with reduced fibers and special fiber a normal toric variety.

The vast majority of $\mathbb{Q}$-Fano varieties are expected to be of class TG.

Conjecture 2. *There is a bijective correspondence between qG-deformation families of $\mathbb{Q}$-Fano threefolds X of class TG and mutation-equivalence classes of rigid maximally mutable Laurent polynomials f in three variables. Under this correspondence the regularized quantum period $\widehat{G}_X$ coincides with the classical period π_f; see §1.1 for more on this.*

Conjecture 2 is a specialisation of [28, Conjecture 5.1] to our three-dimensional setting. As we explain in §1.1, when X and f correspond under Conjecture 2 we expect that there is a qG-degeneration from X to the toric variety X_f defined by the spanning fan of the Newton polytope of f.

Establishing Conjecture 2 will require substantial advances in the Gross–Siebert program [6, 39–43], or in deformation theory (cf. [31, 32]). But nonetheless, whilst the foundations of mirror symmetry are being developed, we can use Conjecture 2 to fill in large parts of the classification of $\mathbb{Q}$-Fano threefolds that were previously unknown. That is, we can use methods inspired by Conjecture 2, and by mirror symmetry more broadly, to *construct* large parts of the

2020 *Mathematics Subject Classification.* 14J33 (Primary); 14J45, 52B20 (Secondary).

Key words and phrases. Mirror symmetry, Fano variety, birational classification, Laurent inversion.

Transactions of the London Mathematical Society, **12**(1) (2025), e70012, doi:10.1112/tlm3.70012

classification. As well as giving many new families of $\mathbb{Q}$-Fano threefolds, these constructions also give supporting evidence for the rich conjectural picture predicted by mirror symmetry.

Our approach is as follows. We first look for rigid maximally mutable Laurent polynomials (MMLPs) [28], by specifying a class of lattice polytopes and then searching algorithmically for all rigid MMLPs f such that the Newton polytope $\operatorname{Newt} f$ lies in this class. Initially here we insist that $\operatorname{Newt} f$ is a three-dimensional lattice polytope with one lattice point in the strict interior; such lattice polytopes are called *canonical* and have been classified [51, 52]. We then expand the search to include certain Laurent polynomials f such that $\operatorname{Newt} f$ has two lattice points in the strict interior [7]. In this way we obtain a large collection of rigid MMLPs in three variables. We partition this set of Laurent polynomials into mutation-equivalence classes and then, for each class, attempt to construct a deformation family of $\mathbb{Q}$-Fano threefolds that realises this class via Conjecture 2. The method – Laurent inversion [30] – that we use to construct X from f is also inspired by mirror symmetry: see §3 below for a detailed discussion, and §4 for several examples.

1.1. **The Mirror Correspondence.** If a $\mathbb{Q}$-Fano threefold X corresponds, via Conjecture 2, to a Laurent polynomial f then the regularized quantum period of X matches the classical period of f [22]. Here the regularized quantum period $\widehat{G}_X$ of X is a generating function

$$\widehat{G}_X(t) = 1 + \sum_{d=2}^{\infty} c_d t^d$$

where $c_d = r_d d!$ and r_d is a certain genus-zero Gromov–Witten invariant of X, and the classical period π_f of $f \in \mathbb{C}[x_1^{\pm 1}, \ldots, x_n^{\pm 1}]$ is

$$\pi_f(t) = \frac{1}{(2\pi i)^n} \int_{(S^1)^n} \frac{1}{1 - tf} \frac{dx_1}{x_1} \cdots \frac{dx_n}{x_n}$$

which expands as a power series

$$\pi_f(t) = \sum_{d=0}^{\infty} \kappa_d t^d$$

with κ_d the coefficient of the constant monomial in f^d. Gromov–Witten invariants are deformation invariant, so the regularized quantum period $\widehat{G}_X$ is a qG-deformation invariant of X. On the other side of the correspondence, the classical period π_f is invariant under mutation of f.

If the Fano variety X corresponds to the Laurent polynomial f via Conjecture 2 then it is expected that there is a qG-degeneration with general fiber X and special fiber X_f, where X_f is the toric variety defined by the spanning fan of the Newton polytope $\operatorname{Newt} f$. Thus one can hope to recover X from the Laurent polynomial f by smoothing the toric variety X_f, which is in general highly singular. The coefficients of f should therefore somehow encode a logarithmic structure [54] on the central fiber X_f of this degeneration. From this perspective one can think of Laurent inversion – the technique that we use to construct $\mathbb{Q}$-Fano threefolds – as attempting to construct the expected smoothing of X_f as an embedded deformation of X_f inside an ambient toric variety built from f. For more on this, see the work of Doran–Harder [36] and also [30, §8]. If the conjectural picture described above, with the $\mathbb{Q}$-Fano variety X degenerating to a toric variety X_f, is correct, then one can think of X as corresponding to a general point on an appropriate component of the Hilbert scheme, and X_f as giving a point on the boundary of that component. From this point of view, the discussion in §4.3 is particularly instructive. We exhibit two rigid MMLPs f_1 and f_2 with the same Newton polytope P – so that $X_{f_1} = X_{f_2} = X_P$ – but different classical periods π_{f_1}, π_{f_2}. We then use Laurent inversion to construct $\mathbb{Q}$-Fano threefolds X_1 and X_2 which correspond respectively to f_1 and f_2 under Conjecture 2. Since the classical periods π_{f_1} and π_{f_2} are different, we have that $\widehat{G}_{X_1} \neq \widehat{G}_{X_2}$; thus X_1 and X_2 are not isomorphic, or even qG-deformation equivalent. This means that X_1 and X_2 lie on different components of the Hilbert scheme, and the singular toric variety X_P lies in the intersection of these components. The choice of rigid MMLP with Newton polytope P – that is, the choice of f_1 or f_2 – corresponds to choosing a component of the Hilbert scheme that contains X_P and gives a smoothing of X_P.

1.2. **The Graded Ring Database.** Miles Reid and his collaborators have pioneered the study of $\mathbb{Q}$-Fano threefolds using graded ring methods [4, 5, 13, 17, 18, 47]. They have determined a set of 39 550 rational functions that contains all Hilbert series of $\mathbb{Q}$-Fano threefolds that satisfy a semistability condition[1] and have Picard rank 1. In practice all known $\mathbb{Q}$-Fano threefolds have Hilbert series contained in this dataset, regardless of semistability or Picard rank, so we will ignore these conditions in what follows. The Hilbert series of a Fano variety X is the generating series for the dimensions of the graded pieces of the anticanonical ring

$$R(X, -K_X) = \bigoplus_{n=0}^{\infty} H^0(X, -nK_X). \tag{1}$$

Note that the Hilbert series is invariant under qG-deformation of X. Choosing a minimal set of homogeneous generators for the anticanonical ring (1) determines an embedding of X into weighted projective space $w\mathbb{P}$, and one can use the Hilbert series to estimate the weights and codimension of such an embedding: see [13, §3]. The Hilbert series also determines the *genus* $g(X) := h^0(X, -K_X) - 2$. When X is smooth, $g(X)$ is the genus of the curve given by intersecting X with two generic hyperplanes in $w\mathbb{P}$.

The dataset of possible Hilbert series is recorded in the Graded Ring Database [10, 12]. One can think of this data as giving a numerical sketch of the possible 'geography' of $\mathbb{Q}$-Fano threefolds. A point to note is that the combinatorial methods used to produce the dataset of possible Hilbert series do not guarantee the existence (or uniqueness) of a deformation family of $\mathbb{Q}$-Fano threefolds with that Hilbert series: there can be zero, one, or many such families. From this point of view, our work gives a new way to approach the realisation problem for a given possible Hilbert series $H(t)$. If there is a $\mathbb{Q}$-Fano threefold X with Hilbert series $H(t)$, and X corresponds under Conjecture 2 to a rigid MMLP f, then as discussed we expect that there is a qG-degeneration from X to the toric variety X_f. This toric variety is defined by the spanning fan of the polytope $P = \operatorname{Newt} f$, and the Hilbert series of X_f is equal to the Ehrhart series of the dual polytope P^*. One can therefore approach the realisation problem as follows.

Given a possible Hilbert series $H(t)$ one can search for Fano polytopes P such that the Ehrhart series of P^* is equal to $H(t)$. For each such P one can search for rigid MMLPs f with Newton polytope P. Partitioning these Laurent polynomials into mutation-equivalence classes predicts the number of deformation families, as well as specific qG toric degenerations X_f of these families. One can then use Laurent inversion (as in §4), or search for toric complete intersection models (as in §5), or use more traditional methods such as unprojection [15, 60] to construct each family.

1.3. **The landscape of $\mathbb{Q}$-Fano threefolds.** Figure 1 gives three different views of the distribution of $\mathbb{Q}$-Fano threefolds:

- Figure 1(a) shows the landscape of possible Hilbert series for $\mathbb{Q}$-Fano threefolds as determined by the Graded Ring Database. Every Hilbert series of a $\mathbb{Q}$-Fano threefold is recorded here, but this analysis is purely numerical and ignores the realisation problem: each Hilbert series here may be represented by zero, one, or many $\mathbb{Q}$-Fano threefolds.
- Figure 1(b) and Figure 1(c) give two views of the landscape assuming the conjectural correspondence between $\mathbb{Q}$-Fano threefolds and mutation-equivalence classes of rigid MMLPs. These are experimental and (necessarily) incomplete. Figure 1(b) records the

[1]See [13] for a precise discussion.

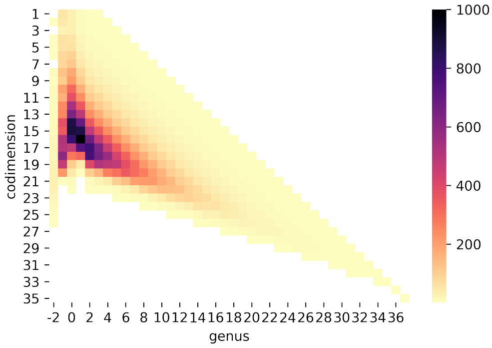

(a) Potential $\mathbb{Q}$-Fano threefolds

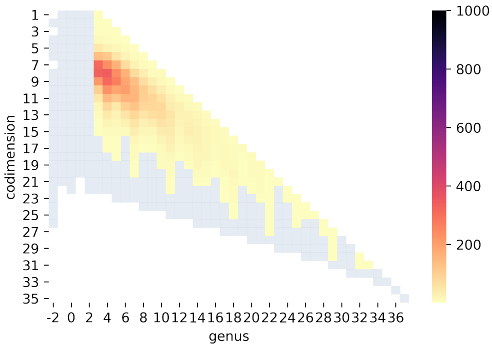

(b) Rigid MMLPs on canonical polytopes

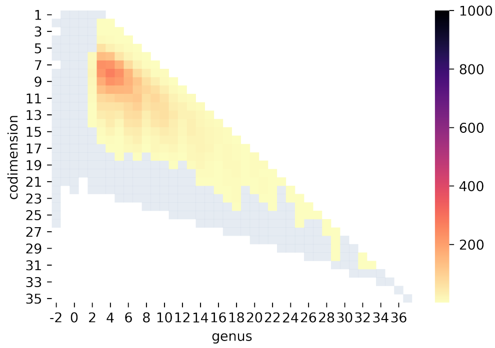

(c) Rigid MMLPs on a sample of 2-point polytopes

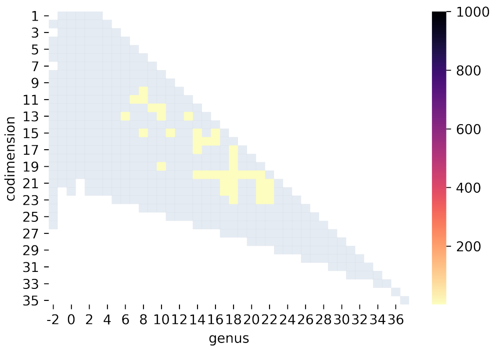

(d) Examples constructed using Laurent inversion

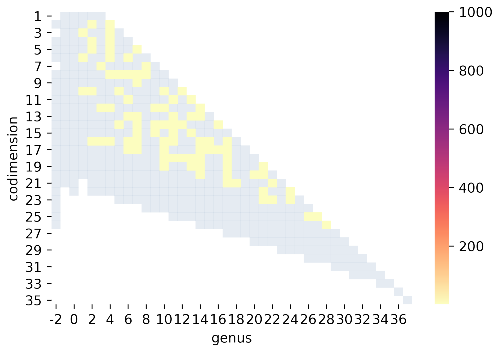

(e) Randomly generated toric hypersurfaces

Figure 1. The distribution of potential Hilbert series for $\mathbb{Q}$-Fano threefolds with Fano index 1: (a) from the Graded Ring Database; (b) from mutation-equivalence classes of rigid MMLPs with three-dimensional canonical Newton polytope; (c) from mutation-equivalence classes of rigid MMLPs with Newton polytope in a random sample of three-dimensional polytopes with two interior points; (d) from toric complete intersections constructed using Laurent inversion; (e) from randomly-generated quasismooth hypersurfaces in toric orbifolds of Picard rank 2. Hilbert series are recorded as pairs (c, g) where c is the estimated codimension and $g = g(X)$ is the genus. Plots (b)–(e) have the shadow of plot (a) as background.

distribution from what we believe to be an almost-complete collection of rigid MMLPs f in three variables such that Newt f is a canonical polytope [27]. Figure 1(c) records the distribution from a random sample of rigid MMLPs in three variables such that Newt f has two interior points.

- Figure 1(d) and Figure 1(e) give two views of the landscape based on genuine $\mathbb{Q}$-Fano threefolds. Figure 1(d) records the distribution from toric complete intersections constructed from rigid MMLPs using Laurent inversion: see §4 and [45]. Figure 1(e) records the distribution from a random sample of quasismooth hypersurfaces in toric orbifolds of Picard rank 2: see §5.

Comparing Figure 1(b) and Figure 1(c) with Figure 1(a) predicts that there are many $\mathbb{Q}$-Fano threefolds with the same Hilbert series, particularly in fairly low codimension and low genus. Comparing Figure 1(c) and Figure 1(e) with Figure 1(b) indicates how restricting the Newton polytope of our rigid MMLPs f to be canonical prevents us from realising parts of the possible $\mathbb{Q}$-Fano landscape: for example it forces $g(X) \geq 3$.

1.4. **Mirror symmetry and the classification of $\mathbb{Q}$-Fano varieties.** The idea that the Fano classification problem can be approached via mirror symmetry was introduced by Corti, Golyshev, and coauthors in the context of smooth Fano varieties [22]. This framework was given substantial support by the analysis of smooth Fano threefolds and their Laurent polynomial mirrors [2,23], and of smooth Fano fourfolds [25,29,48]. Since then, through discussions and work with Corti and his collaborators, further aspects of the story have come into focus: the role of mutation and rigidity [1]; the realisation that the correct setting for the mirror symmetry classification programme is probably $\mathbb{Q}$-Fano varieties rather than smooth Fano varieties [28]; the role of maximally mutable Laurent polynomials (ibid.); and the development of Laurent inversion as a construction technique [30]. In what follows we bring all of this together, formulating a classification program for $\mathbb{Q}$-Fano threefolds from this point of view. Furthermore we draw together techniques that we have used elsewhere, or will use in the future, to begin filling out the $\mathbb{Q}$-Fano threefold classification, illustrating the potential of these methods. This involves advances in Laurent inversion [45] and a new approach that combines Hori–Vafa mirror symmetry [46] in the orbifold setting with a rigidity analysis for MMLPs: see §5.

It is natural to ask how many of the $\mathbb{Q}$-Fano threefolds that we construct in this paper are new. This is a challenging question, because the invariant that we use to distinguish $\mathbb{Q}$-Fano varieties (the regularized quantum period) is built from genus-zero Gromov–Witten invariants; classical construction techniques in birational geometry (unprojection, Sarkisov-style analysis, etc.) are typically not compatible with current techniques for computing Gromov–Witten invariants (degeneration, quantum Lefschetz, Abelianisation, etc.). But we can say something. For example, the 333 randomly-generated examples in §5 together give 130 regularized quantum period sequences, so we expect 130 $\mathbb{Q}$-Fano varieties up to qG-deformation. Of these, 15 are included in the constructions in [45], so we expect that at most 115 of our qG-deformation families are new. Note that the examples constructed via generalised Laurent inversion in [45] are probably not classical because they mostly have very high estimated codimension, whereas classical constructions tend to be in estimated codimension up to six. See Figure 1(d).

2. Maximally Mutable Laurent Polynomials

In this section we define mutations and mutability, and give a criterion (Proposition 8) for a Laurent polynomial to be a rigid MMLP. We then describe our systematic search for rigid MMLPs f in three variables such that the Newton polytope of f is canonical.

2.1. **Mutations.** Let N be a lattice, $M = \mathrm{Hom}(N,\mathbb{Z})$ be the dual lattice, and consider Laurent polynomials $f \in \mathbb{C}[N]$. A *mutation* is an automorphism

$$\begin{aligned} \mu_{w,h}\colon \mathbb{C}(N) &\to \mathbb{C}(N) \\ x^\gamma &\mapsto h^{\langle w,\gamma\rangle} x^\gamma \end{aligned}$$

defined by a primitive lattice vector $w \in M$ called the *weight* and a Laurent polynomial $h \in \mathbb{C}[w^\perp \cap N]$ called the *factor* [2]. Here we can think of w as defining a $\mathbb{Z}$-grading on $\mathbb{C}[N]$, with h lying in the degree-zero piece of that grading. In general, given a Laurent polynomial $f \in \mathbb{C}[N]$, the mutation $g := \mu_{w,h}(f)$ will be a rational function. If $g \in \mathbb{C}[N]$ is also a Laurent polynomial then we say that f is *mutable* with respect to (w,h).

Example 3. Mutability of a Laurent polynomial f imposes constraints on its coefficients. For example, consider the Laurent polynomial

$$f_a = y + \frac{1}{xy} + \frac{a}{y} + \frac{x}{y}$$

in variables x and y, where a is a parameter, and the mutation $\mu_{w,h}\colon \mathbb{C}(N) \to \mathbb{C}(N)$ where $N = \mathbb{Z}^2$, $w = (0,1)$ and $h = 1+x$. Then $\mu_{w,h}$ sends $x \mapsto x$, $y \mapsto (1+x)y$, and f_a is mutable with respect to (w,h) if and only if $a = 2$. To see this, write

$$f_a = y + \frac{1+ax+x^2}{xy}$$

Then f_a is mutable with respect to (w,h) if and only if $1+ax+x^2$ is divisible by $1+x$, that is, if and only if $a = 2$.

Example 4. If the factor h is a monomial, then the mutation $\mu_{w,h}$ is a monomial change of variables and every Laurent polynomial $f \in \mathbb{C}[N]$ is mutable with respect to (w,h), for any weight w. We regard such mutations as trivial: see [28, Definition 2.1].

Example 5. Suppose that $\mu_{w,h}$ is a non-trivial mutation – i.e. h is not a monomial – and that $f \in \mathbb{C}[N]$ is mutable with respect to (w,h). We may choose an identification of N with $\mathbb{Z}^n$ such that the weight $w = (0,\ldots,0,1)$ is the nth standard basis vector for the dual lattice $M = (\mathbb{Z}^n)^\vee$. Write $\mathbb{C}[N] = \mathbb{C}[x_1^{\pm1},\ldots,x_{n-1}^{\pm1},y^{\pm1}]$, so that h is a Laurent polynomial in the variables $x_1,\ldots,x_{n-1}$ and

$$f = \sum_{k=-a}^{b} f_k y^k \tag{2}$$

for some positive integers a, b and some Laurent polynomials f_k in the variables $x_1,\ldots,x_{n-1}$. The mutation $\mu_{w,h} f$ is

$$\mu_{w,h} f = \sum_{k=-a}^{b} h^k f_k y^k$$

and therefore f is mutable if and only if h^k divides f_{-k} for all $k > 0$. Since for any Laurent polynomials g_1, g_2 we have

$$\mathrm{Newt}\left(g_1 g_2\right) = \mathrm{Newt}(g_1) + \mathrm{Newt}(g_2)$$

where the operation on the right-hand side is Minkowski sum of polytopes

$$P_1 + P_2 = \left\{p_1 + p_2 : p_1 \in P_1, p_2 \in P_2\right\}$$

it follows that f is mutable with respect to (w,h) only if the k-fold dilate of $\mathrm{Newt}(h)$ is a Minkowski summand of $\mathrm{Newt}(f_{-k})$ for $1 \le k \le a$.

Definition 6. Consider a Laurent polynomial $f \in \mathbb{C}[N]$ with Newton polytope P:

$$f = \sum_{p \in N \cap P} a_p x^p$$

We will say that f is *normalised* if $a_v = 1$ whenever v is a vertex of P, and that f is *centered* if the origin lies in the strict interior of P and $a_0 = 0$.

Example 7. Consider the polytope P with ID 1523 in the GRDB database of three-dimensional canonical polytopes, as pictured in Figure 2. P has four triangular facets and four hexagonal

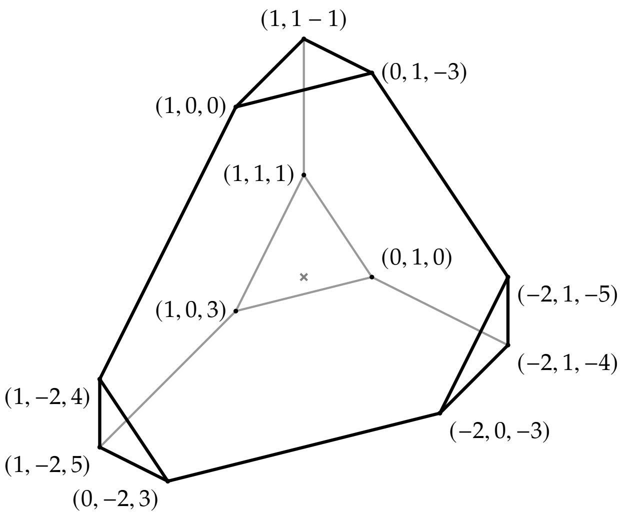

Figure 2. The three-dimensional canonical polytope with GRDB ID 1523.

facets. The automorphism group $\mathrm{Aut}(P)$ is isomorphic to the symmetric group S_4, and acts permuting the hexagonal facets. Let N be the lattice containing P, let $M = \mathrm{Hom}(N, \mathbb{Z})$, and let $w \in M$ be a supporting hyperplane for a hexagonal facet F. The facet F is at height -1 with respect to w, so that if f is a Laurent polynomial with Newton polytope P then the expansion (2) has $a = 1$ (and $b = 2$). There are two distinct Minkowski factorizations of F: see Figure 3. Corresponding to these two Minkowski factorizations, we consider two possible factors h_1 and h_2 for mutations with weight w. In co-ordinates (as in Figure 4) where F is the convex hull of

$$(1, 0), (3, 0), (3, 1), (1, 3), (0, 3), \text{and } (0, 1)$$

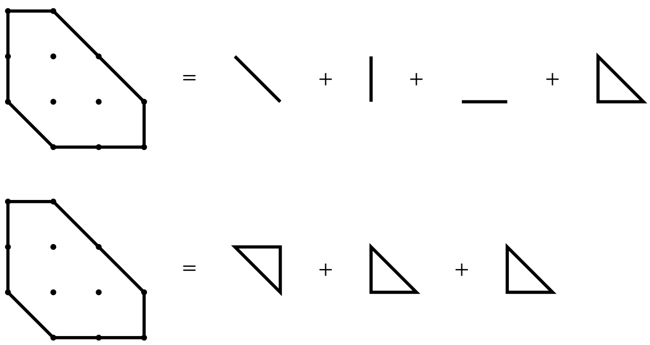

Figure 3. Two different Minkowski decompositions of the facet F.

we have

$$h_1 = (x+y)(1+y)(1+x)(1+x+y)$$
$$h_2 = (x+y+xy)(1+x+y)^2$$

Consider a normalised and centered Laurent polynomial f with $\mathrm{Newt}(f) = P$,

$$f = \sum_{p \in N \cap P} a_p x^p$$

Insisting that f is mutable with respect to (w, h_1) imposes the divisibility condition discussed in Example 5. This fixes the coefficients a_p of lattice points such that $p \in F$ as in Figure 4 and imposes no condition on other coefficients a_p. Similarly, insisting that f is mutable with respect to (w, h_2) fixes the coefficients a_p of lattice points such that $p \in F$ as in Figure 5 and imposes no condition on other coefficients a_p.

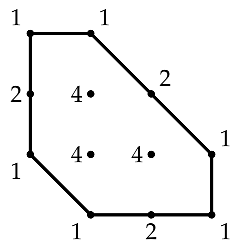

Figure 4. The coefficients a_p, $p \in F$, fixed by mutability with respect to (w, h_1).

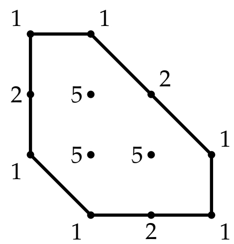

Figure 5. The coefficients a_p, $p \in F$, fixed by mutability with respect to (w, h_2).

Thus fixing, for each hexagonal facet F of P, a choice of h_1 or h_2 defines a set S of four mutations, and there is a unique normalised, centered Laurent polynomial f with $\mathrm{Newt}(f) = P$ such that f is mutable with respect to each element of S. The Laurent polynomial f is a rigid maximally mutable Laurent polynomial [28, Definition 2.6]. In this way we obtain 16 rigid MMLPs, which fall into 5 equivalence classes under the action of $\mathrm{Aut}(P)$.

Given a Laurent polynomial f, write

$$S_f = \{(w, h) : f \text{ is mutable with respect to } (w, h)\}$$

Conversely, given a set S of pairs (w, h) where $w \in M$ is primitive and $h \in \mathbb{C}[w^\perp \cap N]$, write

$$L_P(S) = \left\{ f \in \mathbb{C}[N] : \begin{array}{l} f \text{ is normalised and centered, } \mathrm{Newt}\, f = P, \text{ and } f \text{ is} \\ \text{mutable with respect to } (w, h_{gen}) \text{ for all } (w, h) \in S \end{array} \right\}$$

Here h_{gen} denotes the general normalised Laurent polynomial with the same Newton polytope as h. The following is an immediate consequence of [28, Definition 2.6].

Proposition 8. *Let f be a normalised, centered Laurent polynomial with Newton polytope P and suppose that*

$$L_P(S_f) = \{f\}$$

Then f is a rigid maximally mutable Laurent polynomial.

We believe that the converse to Proposition 8 also holds, that is, that f is a rigid MMLP if and only if $L_P(S_f) = \{f\}$. In forthcoming work, Coates–Kasprzyk–Pitton use this, along with a large-scale computer algebra calculation, to classify rigid MMLPs in three variables with canonical Newton polytope [26], conditional on the converse to Proposition 8.

3. Laurent Inversion and Towers of Bundles

In this section we give a conceptual interpretation of *Laurent inversion* in a special case. Laurent inversion is an algorithmic process for recovering a Fano manifold X from a Laurent polynomial that corresponds to X under mirror symmetry [30]; this process may or may not succeed in any given example. The special case that we analyse, which in practice covers almost all cases in which Laurent inversion has been successfully applied, is where a certain algebraic variety involved, called the *shape variety*, is a tower of projective bundles. The discussion here reformulates and extends ideas that we learned from Charles Doran, Andrew Harder, and Thomas Prince [36,62].

3.1. **The Givental/Hori–Vafa Mirror.** Suppose that Y is a smooth Fano toric orbifold of dimension d. Choosing a numbering of the rays of the fan Σ_Y for Y gives a short exact sequence

$$0 \longrightarrow \mathbb{L} \longrightarrow \mathbb{Z}^r \xrightarrow{\rho} N \longrightarrow 0 \tag{3}$$

where N is a d-dimensional lattice and the map ρ is defined by the rays of Σ_Y. Dualising gives a short exact sequence

$$0 \longleftarrow \mathbb{L}^\vee \xleftarrow{D} (\mathbb{Z}^r)^\vee \longleftarrow M \longleftarrow 0 \tag{4}$$

where $M = N^\vee$. There is a canonical isomorphism $\mathbb{L}^\vee \cong \mathrm{Pic}(Y)$, and the image of the standard basis for $(\mathbb{Z}^r)^\vee$ under the map D gives a numbering $D_1, \ldots, D_r$ of the toric divisors on Y. The Givental/Hori–Vafa mirror [38,46] to Y is the diagram

$$\begin{tikzcd} (\mathbb{Z}^r)^\vee \otimes \mathbb{C}^\times \arrow[r, "W"] \arrow[d, "\pi_D"] & \mathbb{C} \\ \mathbb{L}^\vee \otimes \mathbb{C}^\times & \end{tikzcd} \tag{5}$$

where π_D is the fibration induced by D and $W(x_1, \ldots, x_r) = x_1 + x_2 + \cdots + x_r$.

Suppose now that $L_1, \ldots, L_c$ are line bundles over Y, and that $X \subset Y$ is a quasismooth, well-formed, Fano complete intersection[2] defined by a general section of $L_1 \oplus \cdots \oplus L_c$. Choosing disjoint subsets $S_1, \ldots, S_c$ of $\{1, 2, \ldots, r\}$ such that

$$L_i = \sum_{j \in S_i} D_j \qquad\qquad i \in \{1, 2, \ldots, c\}$$

defines a Givental/Hori–Vafa mirror to X. This is the subvariety of (5) defined by

$$\sum_{j \in S_i} x_j = 1 \qquad\qquad i \in \{1, 2, \ldots, c\}. \tag{6}$$

[2]Quasismooth, well-formed weighted projective complete intersections have been studied by Iano-Fletcher [47]. See [33, Definition 25] for definitions applicable in our context.

3.2. **Towers of bundles.** The equations (6) define a codimension-c subvariety of the total space of the fibration π_D in (5), which we call the *GHV locus*. We will now choose some extra data that allows us to define a toric partial compactification of the GHV locus. This partial compactification arises from an action of $(\mathbb{C}^\times)^c$ on the total space $(\mathbb{Z}^r)^\vee \otimes \mathbb{C}^\times$ of π_D: we realise the codimension-c locus defined by (6) as an open set inside a toric variety $\mathcal{Z} = \big((\mathbb{Z}^r)^\vee \otimes \mathbb{C}\big) /\!\!/ (\mathbb{C}^\times)^c$. The ray sequence for the toric variety $\mathcal{Z}$ and the dual ray sequence (4) for Y fit together as follows:

$$
\begin{tikzcd}
 & & 0 & & & & & \\
 & & & N_{\mathcal{Z}} \arrow[ul] & & & & \\
0 & \mathbb{L}^\vee \arrow[l] & & & (\mathbb{Z}^r)^\vee \arrow[lll, "D"'] \arrow[ul] & & M \arrow[ll, "\rho^T"'] & 0 \arrow[l] \\
 & & & & & \mathbb{Z}^c \arrow[ul] \arrow[ur, dotted] & & \\
 & & & & & & 0 \arrow[ul] &
\end{tikzcd}
\tag{7}
$$

To this end, let $S_0 = \{1, 2, \ldots, r\} \setminus S_1 \cup \cdots \cup S_c$. We will consider a map[3]

$$\zeta : N \longrightarrow (\mathbb{Z}^c)^\vee$$

and write ζ_i for the image under ζ of the ith ray ρ_i of the fan Σ_Y. We will suppose that ζ defines the weight matrix for a tower of projective bundles, that is, if e_j denotes the jth standard basis vector for $\mathbb{Z}^c$ then

$$
\zeta_k(e_j) = \begin{cases} w_{jk} & j < i \text{ or } i = 0 \\ 1 & j = i \\ 0 & j > i \end{cases} \qquad \qquad \text{where } k \in S_i \text{ and } w_{jk} \leq 0.
$$

We call such a map ζ a *tower of bundles* for the complete intersection $X \subset Y$.

If we permute $\{1, 2, \ldots, r\}$ such that $S_0, \ldots, S_c$ occur in that order, i.e. whenever $i \in S_k$ and $j \in S_l$ with $k < l$ we have $i < j$, then the matrix of the composition $\zeta \circ \rho$ takes the form

$$
\begin{pmatrix}
* & \cdots & * & 1 & \cdots & 1 & * & \cdots & * & & * & \cdots & * \\
* & \cdots & * & 0 & \cdots & 0 & 1 & \cdots & 1 & \cdots & * & \cdots & * \\
* & \cdots & * & 0 & \cdots & 0 & 0 & \cdots & 0 & \cdots & \vdots & \cdots & \vdots \\
 & \ddots & & & & & & \ddots & & & * & \cdots & * \\
* & \cdots & * & 0 & \cdots & 0 & 0 & \cdots & 0 & \cdots & 1 & \cdots & 1
\end{pmatrix}
\tag{8}
$$

where $*$ denotes a non-positive integer. Let $n = |S_1| + \cdots + |S_c|$. The last n columns of the matrix above give the weight matrix for an action of $(\mathbb{C}^\times)^c$ on $\mathbb{C}^n$ such that the GIT quotient $\mathbb{C}^n /\!\!/ (\mathbb{C}^\times)^c$, with stability condition $(1, 1, \ldots, 1)$, is a tower of projective bundles $\mathbb{P}$. Each of the first $|S_0|$ columns defines a line bundle $E_i \to \mathbb{P}$ such that the dual bundle $E_i^\vee$ is nef.

The map ζ is closely related to Doran–Harder's notion of *amenable collection* [36], and the tower of projective bundles $\mathbb{P}$ will play the role of the *shape variety* Z from [30]. Thus the discussion which follows gives a geometric interpretation of amenable collections, and clarifies the relationship between the shape variety and Givental/Hori–Vafa mirror symmetry.

[3]The transpose of ζ will be the dotted arrow in (7). The existence of ζ ensures that the action of $(\mathbb{C}^\times)^c$ on $(\mathbb{Z}^r)^\vee \otimes \mathbb{C}$ preserves the fibers of π_D in (5).

3.3. **Partially compactifying the total space of the Givental/Hori–Vafa mirror.** Let ζ be a tower of bundles for the complete intersection $X \subset Y$. Dualising the map $\zeta \circ \rho : \mathbb{Z}^r \to (\mathbb{Z}^c)^\vee$ gives a map $\mathbb{Z}^c \to (\mathbb{Z}^r)^\vee$, and hence a map $\mathbb{Z}^c \otimes \mathbb{C}^\times \to (\mathbb{Z}^r)^\vee \otimes \mathbb{C}^\times$. Thus we obtain an action of $(\mathbb{C}^\times)^c$ on $(\mathbb{Z}^r)^\vee \otimes \mathbb{C}$. Consider the GIT quotient $\mathcal{Z} = \big((\mathbb{Z}^r)^\vee \otimes \mathbb{C}\big) /\!\!/ (\mathbb{C}^\times)^c$, with respect to the stability condition $(1, 1, \ldots, 1)$. This is the total space

$$E = \bigoplus_{i \in S_0} E_i$$

of a direct sum of anti-nef line bundles over $\mathbb{P}$, defined by the first $|S_0|$ columns of the weight matrix (8). In this section we show that E is a partial compactification of the GHV locus (6).

Definition 9. We define functions $\theta_k \colon (\mathbb{Z}^r)^\vee \otimes \mathbb{C} \to \mathbb{C}$ recursively by

$$\theta_k(x) = \sum_{j \in S_k} \left(\prod_{m=1}^{k-1} \theta_m(x)^{-w_{mj}} \right) x_j \qquad\qquad k \in \{1, 2, \ldots, c\}$$

where $x = (x_1, x_2, \ldots, x_r) \in (\mathbb{Z}^r)^\vee \otimes \mathbb{C}$. In particular, $\theta_1(x) = \sum_{j \in S_1} x_j$.

Proposition 10.

(1) *Let $g \in (\mathbb{C}^\times)^c$ and $x \in (\mathbb{Z}^r)^\vee$. The function θ_k satisfies*

$$\theta_k(gx) = \chi_k(g)\theta_k(x)$$

where χ_k is the kth standard character of $(\mathbb{C}^\times)^c$.

(2) *The function θ_k determines a section of the line bundle $L_k \to E$ defined by the character χ_k.*

(3) *The open set U in E defined by*

$$\big(\theta_1 \neq 0, \theta_2 \neq 0, \ldots, \theta_c \neq 0, x_1 \neq 0, x_2 \neq 0, \ldots, x_r \neq 0\big)$$

is isomorphic to the GHV locus (6).

Proof. Part (1) here is a straightforward calculation. Part (2) is a restatement of part (1). For part (3), consider $(x_1, \ldots, x_r) \in (\mathbb{Z}^r)^\vee \otimes \mathbb{C}$ such that $x_1 \neq 0, \ldots, x_r \neq 0$ and $\theta_1 \neq 0, \ldots, \theta_c \neq 0$. The image of $(x_1, \ldots, x_r)$ under the action of $g = (\theta_1^{-1}, \ldots, \theta_c^{-1})$ is $(y_1, \ldots, y_r)$, where

$$y_j = \begin{cases} x_j \theta_k^{-1} \prod_{m=1}^{k-1} \theta_m^{-w_{mj}} & k \neq 0 \\ x_j \prod_{m=1}^{c} \theta_m^{-w_{mj}} & k = 0 \end{cases} \tag{9}$$

and $j \in S_k$. Part (1) now implies that y_j depends only on the $(\mathbb{C}^\times)^c$-orbit of $(x_1, \ldots, x_r)$. Since

$$\sum_{j \in S_k} y_j = 1 \qquad\qquad j \in \{1, 2, \ldots, c\}$$

we see that mapping $(x_1, \ldots, x_r)$ to $(y_1, \ldots, y_r)$ defines a map ϕ from the open set U to the locus (6). Setting $x_j = y_j$ defines an inverse to ϕ; this completes the proof. □

Proposition 11. *The function W from (6), which in view of Proposition 10 can be regarded as a function on U, extends holomorphically across the locus*

$$(\theta_1 = 0, \ldots, \theta_k = 0)$$

in E.

Proof. By construction

$$W = \sum_{j \in S_0} y_j + c$$

on U. The result now follows from (9), because $w_{mj} \leq 0$ for all m and j. □

3.4. **Laurent polynomial mirrors.** In the approach to the classification of Fano varieties pioneered by Corti and Golyshev, Fano varieties of dimension n conjecturally correspond to equivalence classes of Laurent polynomials in n variables [22]. This correspondence is an instance of mirror symmetry. If X is a Fano toric variety then a Laurent polynomial f that corresponds to X under mirror symmetry can be obtained from the Givental/Hori–Vafa mirror by restriction to a fiber, as follows. In the notation of §3.1 we take $X = Y$ and $c = 0$, so that the set of equations (6) is empty. The Givental/Hori–Vafa mirror to X is then the diagram (5). The Laurent polynomial f arises by restricting the superpotential W to the fiber of π_D over the identity element in $\mathbb{L}^\vee \otimes \mathbb{C}^\times$. From the exact sequence (4) we see that this fiber is canonically identified with $M \otimes \mathbb{C}^\times$. The restriction of W to this fiber is given by

$$f = \sum_{i=1}^{r} x^{\rho_i}$$

where $\rho_i \in N$ is the ith ray of the fan for X. Here x^{ρ_i} arises as restriction of the function x_i to the fiber of π_D over the identity element; put differently, x^{ρ_i} arises as the image of x_i (which is the function on $(\mathbb{Z}^r)^\vee \otimes \mathbb{C}^\times$ given by the ith standard basis element in $\mathbb{Z}^r$) under the ray map ρ in (3). Since $\operatorname{rk} M = \dim X = n$, we see that f is a Laurent polynomial in n variables.

If X is a Fano toric complete intersection (as opposed to a toric variety) then the process of obtaining a Laurent polynomial from the Givental/Hori–Vafa mirror is more involved. It amounts to choosing a *torus chart* – an open set birational to an n-dimensional torus – on the fiber of the locus (6) over the identity element, such that the restriction of the superpotential W to this open set is a Laurent polynomial. As we will explain in the next section, one way to construct such a torus chart arises from a tower of bundles that satisfy an additional condition.

3.5. **Partially compactifying the fiber of the Givental/Hori–Vafa mirror.** In §3.3 we described how a tower of bundles gives rise to a partial compactification of the GHV locus. In this section we give a refinement of this construction which preserves the fibration structure given by π_D in (6). That is, we construct a fiberwise partial compactification of the GHV locus. As promised, this also gives a torus chart on the fiber of π_D over the identity element of $\mathbb{L}^\vee \otimes \mathbb{C}^\times$. The key ingredient is a tower of bundles that contains a basis.

Definition 12. We say that a tower of bundles for the toric complete intersection $X \subset Y$ *contains a basis* if the set of toric divisors $\{D_i : i \in S_0\}$ contains a basis for the lattice $\operatorname{Pic}(Y)$.

Consider a tower of bundles for the toric complete intersection $X \subset Y$ that contains a basis. Let $B \subset S_0$ be such that $\{D_j : j \in B\}$ is a basis for $\operatorname{Pic}(Y)$. Without loss of generality we may permute $\{1, 2, \ldots, r\}$ such that whenever $i \in S_k$ and $j \in S_l$ with $k < l$ we have $i < j$, and that $B = \{1, 2, \ldots, |B|\}$. The ray sequence (3) and the tower of bundles together give a diagram:

$$\begin{tikzcd} 0 \arrow[r] & \mathbb{L} \arrow[r, "D^T"] & \mathbb{Z}^r \arrow[r, "\rho"] \arrow[dr] & N \arrow[r] \arrow[d, "\zeta"] & 0 \\ & & & (\mathbb{Z}^c)^\vee & \end{tikzcd} \tag{10}$$

Write $B' = \{1, 2, \ldots, r\} \setminus B$, so that $\mathbb{Z}^r = \mathbb{Z}^B \oplus \mathbb{Z}^{B'}$, and let $p_B : \mathbb{Z}^r \to \mathbb{Z}^B$ denote the projection. Our assumptions about the basis guarantee both that $p_B \circ D^T$ is an isomorphism and that $\{\rho_j : j \in B'\}$ is a basis for N. Thus there are (unique) identifications of $\mathbb{L}$ with $\mathbb{Z}^B$ and N with $\mathbb{Z}^{B'}$ such that in the diagram

$$\begin{tikzcd} 0 \arrow[r] & \mathbb{Z}^B \arrow[r, "D^T"] & \mathbb{Z}^r \arrow[rr, "\rho"] \arrow[dr] & & \mathbb{Z}^{B'} \arrow[r] \arrow[dl, "\zeta"] & 0 \\ & & & (\mathbb{Z}^c)^\vee & & \end{tikzcd} \tag{11}$$

induced from (10), both $p_B \circ D^T$ and $\rho|_{\mathbb{Z}^{B'}}$ are identity maps. Thus a tower of bundles with a basis gives splittings in two different senses:

(a) a splitting $\mathbb{Z}^{B'} \to \mathbb{Z}^r$ of the ray map ρ, and hence of the ray sequence (3);
(b) a splitting $N \otimes \mathbb{C}^\times \cong \mathbb{Z}^{B'} \otimes \mathbb{C}^\times$ of the torus $N \otimes \mathbb{C}^\times$.

Splitting (b) here is equivalent, by duality, to:

(b′) a splitting $M \otimes \mathbb{C}^\times \cong (\mathbb{Z}^{B'})^\vee \otimes \mathbb{C}^\times$ of the torus $M \otimes \mathbb{C}^\times$.

Recall that $M \otimes \mathbb{C}^\times$ is the fiber of the Givental/Hori–Vafa mirror (5) for the ambient space Y.

Consider now the mirror fibration π_D from (5). This is a principal $M \otimes \mathbb{C}^\times$-bundle

$$\begin{tikzcd} M \otimes \mathbb{C}^\times \arrow[r] & (\mathbb{Z}^r)^\vee \otimes \mathbb{C}^\times \arrow[d, "\pi_D"] \\ & \mathbb{L}^\vee \otimes \mathbb{C}^\times \end{tikzcd} \tag{12}$$

and splitting (b′) identifies this with a principal $(\mathbb{Z}^{B'})^\vee \otimes \mathbb{C}^\times$-bundle. Since it is split, the torus $(\mathbb{Z}^{B'})^\vee \otimes \mathbb{C}^\times$ acts canonically on the vector space $(\mathbb{Z}^{B'})^\vee \otimes \mathbb{C} = (\mathbb{C}^{B'})^\vee$. We form the associated vector bundle to (12) with fiber $(\mathbb{C}^{B'})^\vee$; this is a vector bundle $\mathcal{V} \to \mathbb{L}^\vee \otimes \mathbb{C}^\times$ of rank $|B'|$. The vector bundle $\mathcal{V}$ carries a fiberwise action of $(\mathbb{C}^\times)^c$, given by dualising the map ζ in (11).

Definition 13. Let $\mathcal{Z}$ denote the GIT quotient $\mathcal{V} /\!\!/ (\mathbb{C}^\times)^c$ with stability condition $(1, 1, \ldots, 1)$, and let Z denote the fiber of $\mathcal{Z} \to \mathbb{L}^\vee \otimes \mathbb{C}^\times$ over the identity element $e \in \mathbb{L}^\vee \otimes \mathbb{C}^\times$.

Proposition 14.

(1) $\mathcal{Z}$ is an open subset of the partial compactification E defined in §3.3;
(2) $\mathcal{Z}$ is a fiberwise partial compactification of the GHV locus (6);
(3) the fiber Z is a toric variety;
(4) if $S_0 = B$ then Z is isomorphic to $\mathbb{P}$, the tower of projective bundles defined in §3.2;
(5) if S_0 strictly contains B then Z is isomorphic to the total space of the direct sum of anti-nef line bundles over $\mathbb{P}$ defined by the columns of (8) indexed by $S_0 \setminus B$.

Proof. The splitting (a) shows that the principal $M \otimes \mathbb{C}^\times$-bundle (12) is in fact trivial:

$$\begin{tikzcd} (\mathbb{Z}^{B'})^\vee \otimes \mathbb{C}^\times \arrow[r] & (\mathbb{Z}^r)^\vee \otimes \mathbb{C}^\times \arrow[d, "\pi_D"] \\ & (\mathbb{Z}^B)^\vee \otimes \mathbb{C}^\times \end{tikzcd}$$

Thus $(\mathbb{Z}^r)^\vee \otimes \mathbb{C}$ contains the total space of $\mathcal{V}$ as an open set. The embedding of $\mathcal{V}$ into $(\mathbb{Z}^r)^\vee \otimes \mathbb{C}$ respects the action of $(\mathbb{C}^\times)^c$, so this proves (1).

To prove (2), we argue exactly as in Proposition 10. Fix $q \in \mathbb{L}^\vee \otimes \mathbb{C}^\times$ and consider the fiber $\mathcal{V}_q$ of the vector bundle $\mathcal{V}$ over q. The splitting (b′) gives rise to distinguished co-ordinates $(x_j : j \notin B)$, on $\mathcal{V}_q$, and we define[4] functions $\theta_k : \mathcal{V}_q \to \mathbb{C}$ exactly as in Definition 9:

$$\theta_k(x) = \sum_{j \in S_k} \left(\prod_{m=1}^{k-1} \theta_m(x)^{-w_{mj}} \right) x_j \qquad k \in \{1, 2, \ldots, c\}$$

Consider functions y_j defined as in (9):

$$y_j = \begin{cases} x_j \theta_k^{-1} \prod_{m=1}^{k-1} \theta_m^{-w_{mj}} & k \neq 0 \\ x_j \prod_{m=1}^{c} \theta_m^{-w_{mj}} & k = 0 \end{cases} \qquad j \notin B$$

where k is such that $j \in S_k$. The open set $\tilde{U} \subset \mathcal{V}_q$ defined by

$$(\theta_1 \neq 0, \theta_2 \neq 0, \ldots, \theta_c \neq 0) \cap (x_j \neq 0 : j \notin B)$$

projects to an open set U in the quotient $\mathcal{V}_q /\!\!/ (\mathbb{C}^\times)^c$, and the map

$$\begin{aligned} \tilde{\phi} : \tilde{U} &\longrightarrow (\mathbb{Z}^{B'})^\vee \otimes \mathbb{C}^\times \\ (x_j : j \notin B) &\longmapsto (y_j : j \notin B) \end{aligned} \tag{13}$$

descends to give a well-defined map ϕ from U to the subset of $(\mathbb{Z}^{B'})^\vee \otimes \mathbb{C}^\times$ defined by

$$\sum_{j \in S_i} y_j = 1 \qquad i \in \{1, 2, \ldots, c\}.$$

The map ϕ is an isomorphism, with inverse given by setting $x_j = y_j$, $j \notin B$. Thus the Givental/Hori–Vafa locus (6) embeds into $\mathcal{Z}$ as an open set, and this embedding exhibits $\mathcal{Z}$ as a fiberwise partial compactification of (6).

Part (3) is obvious, as Z is the GIT quotient $\mathcal{V}_e /\!\!/ (\mathbb{C}^\times)^k$. To identify this quotient, we examine the weights of the $(\mathbb{C}^\times)^k$-action on the fiber. These are the entries in the matrix of the map ζ in diagram (11), with respect to the standard bases for $\mathbb{Z}^{B'}$ and $(\mathbb{Z}^c)^\vee$. This matrix is given by the last $|B'|$ columns of (8). If $S_0 = B$ then this is

$$\begin{pmatrix} 1 & \cdots & 1 & * & \cdots & * & \cdots & * & \cdots & * \\ 0 & \cdots & 0 & 1 & \cdots & 1 & \cdots & * & \cdots & * \\ 0 & \cdots & 0 & 0 & \cdots & 0 & \cdots & \vdots & \cdots & \vdots \\ & & & & \ddots & & & * & \cdots & * \\ 0 & \cdots & 0 & 0 & \cdots & 0 & \cdots & 1 & \cdots & 1 \end{pmatrix}$$

which proves (4). Otherwise there are an additional $|S_0 \setminus B|$ leading columns, all of which contain non-positive entries; this proves (5). ◻

3.6. **Laurent polynomials and scaffoldings from towers of bundles.** In §3.5 we constructed a toric partial compactification Z of the fiber of the Givental/Hori–Vafa mirror to a toric complete intersection $X \subset Y$. In this section we explain how this gives rise to a Laurent polynomial f that corresponds to X under mirror symmetry (see §3.4). The Laurent polynomial f arises as a function on the dense torus in Z, and comes equipped with a *scaffolding* [30]. This is a decomposition of f into summands, called *struts*, of a specific form.

The superpotential W in the Givental/Hori–Vafa mirror restricts to the locus (6) to give

$$W = \sum_{j \in S_0} y_j + c$$

(cf. Proposition 11), and restricts to the fiber over $e \in \mathbb{L}^\vee \otimes \mathbb{C}^\times$ to give

$$W = \sum_{j \in S_0} y^{\rho_j} + c$$

[4]Or, equivalently, we could restrict the functions $\theta_k : (\mathbb{Z}^r)^\vee \otimes \mathbb{C} \to \mathbb{C}$ from Definition 9 to $\mathcal{V}_q$ via the embedding $\mathcal{V} \to (\mathbb{Z}^r)^\vee \otimes \mathbb{C}$ just discussed.

where $\rho_j \in N$ is the jth ray of the fan for Y. To obtain a meromorphic function on Z, we first pull W back to the open set $\tilde{U} \subset \mathcal{V}_e$ along the map (13), finding

$$\tilde{\phi}^*(W) = \sum_{j \in S_0} x^{\rho_j} \prod_{m=1}^{c} \theta_m^{-w_{mj}} + c \tag{14}$$

The function $\tilde{\phi}^*(W)$ is invariant under the action of $(\mathbb{C}^\times)^c$ by construction – and indeed we see that each summand on the right-hand side of (14) is homogeneous of weight zero – and so (14) descends to give a well-defined function $\phi^*(W)$ on $U \subset Z$. As in Proposition 11, the function $f := \phi^* W$ extends holomorphically across the locus

$$(\theta_1 = 0, \ldots, \theta_k = 0)$$

in Z, and thus defines a holomorphic function on the dense torus in Z.

We want to regard the function f as a Laurent polynomial. That is, we want to construct a splitting of the dense torus

$$T_Z = \left((\mathbb{Z}^{B'})^\vee \otimes \mathbb{C}^\times \right) / (\mathbb{C}^\times)^c$$

in Z. Such a splitting will give distinguished co-ordinates on T, and expressing f in terms of these co-ordinates will yield a Laurent polynomial. Choose a set F made up of one element from each S_i, $i \in \{1, 2, \ldots, c\}$. Then

$$T_Z \cong (\mathbb{Z}^{B' \setminus F})^\vee \otimes \mathbb{C}^\times.$$

To express f in these co-ordinates, we take the expression (14) and set $x_j = 1$ for all $j \in F$. The result is a Laurent polynomial in variables

$$\{x_j : j \in B', j \notin F\}$$

Each summand $x^{\rho_j} \prod_{m=1}^{c} \theta_m^{-w_{mj}}$ in (14) gives a strut, and so f comes with a distinguished scaffolding.

Remark 15. In the original work on Laurent inversion [30], the struts in a scaffolding are polytopes of sections of nef line bundles on a toric variety called the shape variety. Here we consider struts as specific sections of line bundles on the toric variety Z. That these line bundles are nef follows from the fact that $\prod_{m=1}^{c} \theta_m^{-w_{mj}}$ is a section of the line bundle $E_j^\vee \to Z$ where the dual bundle $E_j \to Z$ is defined by the jth column of the weight matrix (8). Since $w_{mj} \leq 0$ for all m and j, the line bundle $E_j^\vee \to Z$ is nef.

Remark 16. Recall that, if a Laurent polynomial f corresponds under mirror symmetry to a Fano variety X, then it is expected that there is a qG-degeneration with general fiber X and special fiber the toric variety X_f. In our situation Doran–Harder have constructed an embedded degeneration [36] of the complete intersection X to the toric subvariety of Y defined, in Cox co-ordinates $(z_i)_{i=1}^r$, by the binomials

$$\prod_{j \in S_i} z_j = \prod_{j \notin S_i} z_j^{-w_{ij}} \qquad i \in \{1, 2, \ldots, c\}$$

This is the expected degeneration of X to X_f [30, Proposition 12.2].

Example 17. Let X denote a complete intersection of type $(1,1)\cdot(1,1)$ in $Y=\mathbb{P}^2\times\mathbb{P}^2$, and write the ray sequence (3) for Y as

$$0 \longrightarrow \mathbb{Z}^2 \xrightarrow{\begin{pmatrix}1&0\\0&1\\1&0\\0&1\\1&0\\0&1\end{pmatrix}} \mathbb{Z}^6 \xrightarrow{\begin{pmatrix}-1&0&1&0&0&0\\-1&0&0&0&1&0\\0&-1&0&1&0&0\\0&-1&0&0&0&1\end{pmatrix}} \mathbb{Z}^4 \longrightarrow 0$$

Set $S_0=\{1,2\}$, $S_1=\{3,4\}$, $S_2=\{5,6\}$, and consider a weight matrix (8) for a tower of bundles:

$$\begin{pmatrix}*&*&1&1&0&-a\\ *&*&0&0&1&1\end{pmatrix}$$

Solving for the leftmost two columns, using the fact that the weight matrix left-annihilates the first matrix in the ray sequence, yields

$$\begin{pmatrix}-1&a-1&1&1&0&-a\\ -1&-1&0&0&1&1\end{pmatrix}$$

and since we need $a-1\leq 0$ and $-a\leq 0$ it follows that a must be either 0 or 1. Both choices give a tower of bundles with basis, and in each case $S_0=B$. We have:

$$\begin{aligned}\theta_1 &= x_3+x_4\\ \theta_2 &= x_5+(x_3+x_4)^a x_6\end{aligned}$$

The pullback (14) is

$$\frac{(x_3+x_4)(x_5+(x_3+x_4)^a x_6)}{x_3x_5}+\frac{(x_3+x_4)^{1-a}(x_5+(x_3+x_4)^a x_6)}{x_2x_4}+2$$

and we regard this as a Laurent polynomial by setting

$$x_3=1 \qquad x_4=x \qquad x_5=1 \qquad x_6=y$$

obtaining either

$$f=(1+x)(1+y)+\frac{(1+x)(1+y)}{xy}+2$$

if $a=0$, or

$$f=(1+x)(1+(1+x)y)+\frac{1+(1+x)y}{xy}+2$$

if $a=1$. The two Newton polytopes are shown, together with the Newton polytopes of the struts, in Figure 6. It is striking that the two Laurent polynomials, and scaffoldings, that result differ by a mutation [2].

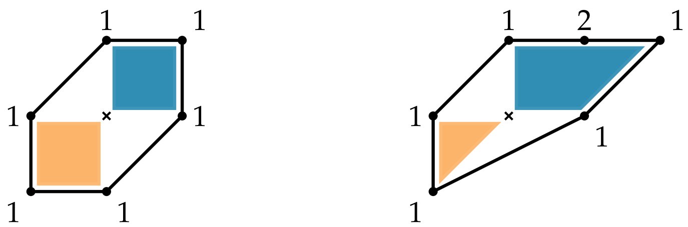

Figure 6. The scaffoldings arising from towers of bundles in Example 17.

3.7. **Reconstructing toric complete intersections from scaffoldings.** Laurent inversion in this context amounts to the assertion that the construction in §3.6 is reversible: that we can reconstruct $X \subset Y$ and the tower of bundles from the resulting Laurent polynomial f and its scaffolding. This is clear. From the scaffolding one can read off the functions $\theta_k(x)$, or more precisely the restrictions

$$\theta_k(x)\big|_{x_j = 1 \text{ for } j \in F} \qquad\qquad k \in \{1, 2, \ldots, c\}.$$

In particular this determines the weights w_{jk} in the weight matrix (8) with k in $S_1 \cup S_2 \cup \cdots \cup S_c$. These are the shaded weights here:

$$\begin{pmatrix}
* & \cdots & * & 1 & \cdots & 1 & * & \cdots & * & & * & \cdots & * \\
* & \cdots & * & 0 & \cdots & 0 & 1 & \cdots & 1 & \cdots & * & \cdots & * \\
* & \cdots & * & 0 & \cdots & 0 & 0 & \cdots & 0 & \cdots & \vdots & \cdots & \vdots \\
 & \ddots & & & & & & \ddots & & & * & \cdots & * \\
* & \cdots & * & 0 & \cdots & 0 & 0 & \cdots & 0 & \cdots & 1 & \cdots & 1
\end{pmatrix}$$

The remaining weights are determined by the powers of θ_k that occur in the struts, and so the scaffolding determines the entire weight matrix (8). The Laurent polynomial f is the restriction of (14):

$$f = c + \sum_{j \in S_0} x^{\rho_j} \prod_{m=1}^{c} \theta_m^{-w_{mj}} \Big|_{x_j = 1 \text{ for } j \in F}$$

But before restriction, each term in (14) is homogeneous of degree zero, and we have already reconstructed the matrix of weights. Thus

$$\tilde{\phi}^*(W) = c + \sum_{j \in S_0} x^{\rho_j} \prod_{m=1}^{c} \theta_m^{-w_{mj}}$$

can be uniquely reconstructed from f by homogeneity. This determines the rays ρ_j, $j \in S_0$, of the fan for Y; since the other rays are the standard basis for $N \cong \mathbb{Z}^{B'}$ and the toric variety Y is Fano by assumption, this completely determines Y. Furthermore the weight matrix (8) determines the subsets $S_1, \ldots, S_c$, and hence the line bundles $L_1, \ldots, L_c$. Thus we can reconstruct the presentation of X as a toric complete intersection $X \subset Y$ from the scaffolding of f.

4. Constructions via Laurent inversion

In this section we apply the reconstruction procedure developed in §3.7 to several concrete examples.

4.1. **Basic example.** Consider the Laurent polynomial

$$f = x + y + \frac{x}{y} + \frac{2}{y} + \frac{1}{xy} + \frac{2}{x} + \frac{y}{x}$$

with scaffolding

$$f = \frac{(x+y+1)^2}{xy} + (x+y+1) - 3$$

The Newton polytope P of f is as pictured in Figure 7. To reconstruct a toric intersection from the scaffolding, we proceed as in §3.7. We find $c = 1$, and

$$\theta_1(x, y) = 1 + x + y.$$

Thus $|S_1| = 3$. Changing the constant term of f does not affect the Fano manifold that corresponds to X under mirror symmetry, so we consider

$$f = 1 + \frac{(x+y+1)^2}{xy} + (x+y+1)$$

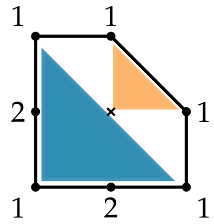

Figure 7. A scaffolding of f with shape $\mathbb{P}^2$.

This gives $|S_0| = 2$, and the weight matrix (8) as

$$\begin{pmatrix} -2 & -1 & 1 & 1 & 1 \end{pmatrix}$$

In co-ordinates $(x_1, x_2, x_3, x_4, x_5)$ with $x_4 = x$ and $x_5 = y$, we see that f homogenises to

$$1 + \frac{(x_3 + x_4 + x_5)^2}{x_4 x_5} + \frac{x_3 + x_4 + x_5}{x_3}$$

which is (14). Thus the ray map ρ in (11) has matrix

$$\begin{pmatrix} 0 & -1 & 1 & 0 & 0 \\ -1 & 0 & 0 & 1 & 0 \\ -1 & 0 & 0 & 0 & 1 \end{pmatrix}$$

and the weight matrix D for the toric variety Y is

$$\begin{pmatrix} 1 & 0 & 0 & 1 & 1 \\ 0 & 1 & 1 & 0 & 0 \end{pmatrix} \tag{15}$$

We see that Y is $\mathbb{P}^2 \times \mathbb{P}^1$, and that X is cut out of Y by a section of $\sum_{j \in S_1} D_j = \mathcal{O}(2, 1)$.

Fix Cox co-ordinates $(z_1, z_2, z_3, z_4, z_5)$ on Y compatible with (15), so that $[z_1 : z_4 : z_5]$ are projective co-ordinates on $\mathbb{P}^2$ and $[z_2 : z_3]$ are projective co-ordinates on $\mathbb{P}^1$. Then X_P is cut out of Y by the binomial section

$$z_1^2 z_2 = z_3 z_4 z_5$$

of $\mathcal{O}(2, 1)$, by Remark 16, and this smooths to a general section

$$f_2(z_1, z_4, z_5) z_2 + g_2(z_1, z_4, z_5) z_3$$

of $\mathcal{O}(2, 1)$, where f_2 and g_2 are polynomials of degree two. Projecting to the first factor $\mathbb{P}^2$ of $Y = \mathbb{P}^2 \times \mathbb{P}^1$ exhibits the hypersurface $X \subset Y$ as the blow-up of $\mathbb{P}^2$ in four points.

4.2. **Wedge shapes.** Another scaffolding of the Laurent polynomial

$$f = x + y + \frac{x}{y} + \frac{2}{y} + \frac{1}{xy} + \frac{2}{x} + \frac{y}{x}$$

from §4.1 is

$$f = \frac{(1+x)^2 + (1+x)y}{x} + \frac{(1+x)^2 + (1+x)y}{xy} - 3$$

The Newton polytopes of f and these struts are pictured in Figure 8. Reconstructing toric complete intersection data as in §3.7, we find that $c = 2$, and

$$\theta_1(x, y) = 1 + x$$
$$\theta_2(x, y) = (1+x)^2 + (1+x)y$$

Thus $|S_1| = |S_2| = 2$. Changing the constant term of f, as before, we consider

$$f = 2 + \frac{(1+x)^2 + (1+x)y}{x} + \frac{(1+x)^2 + (1+x)y}{xy}$$

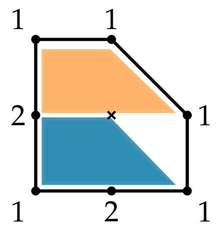

Figure 8. A scaffolding of f with shape $\mathbb{F}_1$.

This gives $|S_0| = 2$, and the weight matrix (8) as

$$\begin{pmatrix} 0 & 0 & 1 & 1 & -2 & -1 \\ -1 & -1 & 0 & 0 & 1 & 1 \end{pmatrix}$$

In co-ordinates $(x_1, x_2, x_3, x_4, x_5, x_6)$ with $x_4 = x$ and $x_6 = y$, we see that f homogenises to

$$2 + \frac{(x_3 + x_4)^2 x_5 + (x_3 + x_4)x_6}{x_3 x_4 x_5} + \frac{(x_3 + x_4)^2 x_5 + (x_3 + x_4)x_6}{x_4 x_6}$$

which is (14). The ray map ρ in (11) therefore has matrix

$$\begin{pmatrix} -1 & 0 & 1 & 0 & 0 & 0 \\ -1 & -1 & 0 & 1 & 0 & 0 \\ -1 & 0 & 0 & 0 & 1 & 0 \\ 0 & -1 & 0 & 0 & 0 & 1 \end{pmatrix}$$

and the weight matrix D for the toric variety Y is

$$\begin{pmatrix} 1 & 0 & 1 & 1 & 1 & 0 \\ 0 & 1 & 0 & 1 & 0 & 1 \end{pmatrix} \tag{16}$$

The line bundles here are

$$L_1 = \sum_{j \in S_1} D_j = \mathcal{O}(1, 2) \qquad\qquad L_2 = \sum_{j \in S_2} D_j = \mathcal{O}(1, 1)$$

and X is cut out of the toric variety Y by a section of $L_1 \oplus L_2$.

Note that L_2 coincides with the toric divisor D_4 given by the fourth column of the weight matrix (16). A general section s_2 of L_2, in Cox co-ordinates $(z_1, z_2, z_3, z_4, z_5, z_6)$ on Y compatible with (16), is

$$z_1 z_2 + z_1 z_6 + z_2 z_1 + z_2 z_5 + z_3 z_6 + z_4 + z_5 z_6$$

where we omit general coefficients from the equation. Thus we can solve $s_2 = 0$ for z_4, eliminating both the fourth column of (16) and the line bundle L_2, and recovering the weight matrix for $\mathbb{P}^1 \times \mathbb{P}^2$ and the line bundle $L_1 = \mathcal{O}(1, 2)$ as in the previous example.

4.3. **Two rigid MMLPs with the same Newton polytope.** Consider the following Laurent polynomials:

$$f_1 = x + yz + y + \frac{y}{x} + \frac{z}{x} + \frac{2}{x} + \frac{1}{xz} + \frac{z}{xy} + \frac{2}{xy} + \frac{1}{xyz}$$
$$f_2 = x + yz + y + \frac{y}{x} + \frac{z}{x} + \frac{3}{x} + \frac{1}{xz} + \frac{z}{xy} + \frac{2}{xy} + \frac{1}{xyz}$$

These have the same Newton polytope P, pictured in Figure 9 below; this is a canonical polytope, and is $GL(3, \mathbb{Z})$-equivalent to the three-dimensional canonical polytope with ID 427129 in the the Graded Ring Database [11].

If X is a $\mathbb{Q}$-Fano 3-fold that corresponds under mirror symmetry to either f_1 or f_2 then, as discussed, we expect that there is a qG-degeneration with general fiber X and special fiber X_P.

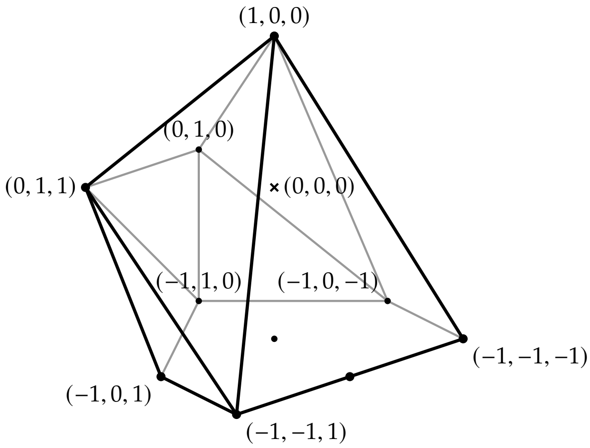

Figure 9. The Newton polytope P for f_1 and f_2.

In particular, therefore, the Hilbert series of X will coincide with the Hilbert series of X_P. The singularities of any $\mathbb{Q}$-Fano 3-fold are determined by its Hilbert series [5, 13], and in this case this suggests that X should have exactly two singularities, both of type $\frac{1}{2}(1, 1, 1)$.

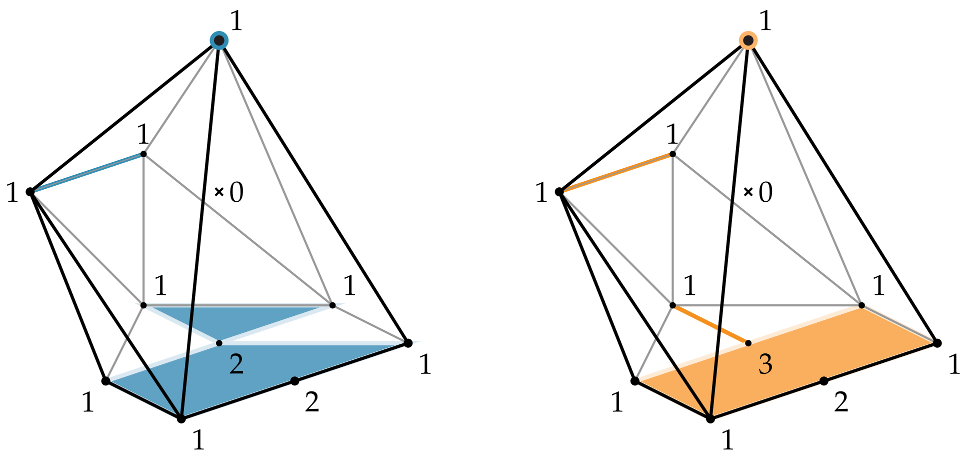

Figure 10. Scaffoldings of f_1 and f_2.

Consider the scaffoldings of f_1 and f_2 shown in Figure 10; the scaffolding of f_1 has shape $\mathbb{F}_1$ and the scaffolding of f_2 has shape $\mathbb{P}^1 \times \mathbb{P}^1$. In each case $|S_0 \setminus B| = 1$ and the vertex of P corresponding to the element of $S_0 \setminus B$ is indicated with a circle. As we will see, applying Laurent inversion to these scaffoldings produces toric complete intersections $X_1 \subset Y_1$ and $X_2 \subset Y_2$ such that Y_1 and Y_2 are toric orbifolds. Each of the varieties X_1 and X_2 is a $\mathbb{Q}$-Fano 3-fold with singular locus consisting of exactly two singularities of type $\frac{1}{2}(1, 1, 1)$. The varieties X_1 and X_2 are not isomorphic (or even deformation equivalent) to each other, because they have distinct quantum periods.

4.3.1. *The scaffolding of f_1.* Here

$$f_1 = (1 + z^{-1})yz + \frac{(1 + z^{-1})(1 + z^{-1} + y)z}{xy} + \frac{1 + z^{-1} + y}{x} + x$$

which, after the change of variables $z \mapsto z^{-1}$, gives

$$\frac{(1 + z)y}{z} + \frac{(1 + z)(1 + z + y)}{xyz} + \frac{1 + z + y}{x} + x$$

Following §3.7 again, we find that $c = 2$ and

$$\theta_1(x,y,z) = 1 + z$$
$$\theta_2(x,y,z) = 1 + z + y$$

Thus $|S_1| = |S_2| = 2$. Shifting the constant term, as before, we consider

$$2 + \frac{(1+z)y}{z} + \frac{(1+z)(1+z+y)}{xyz} + \frac{1+z+y}{x} + x$$

This gives $|S_0| = 4$, and the weight matrix (8) as

$$\begin{pmatrix} -1 & -1 & 0 & 0 & 1 & 1 & -1 & 0 \\ 0 & -1 & -1 & 0 & 0 & 0 & 1 & 1 \end{pmatrix}$$

In co-ordinates $(x_1, x_2, \ldots, x_8)$ with $x_4 = x$, $x_6 = z$, and $x_8 = y$ we see that f homogenises to

$$2 + \frac{(x_5+x_6)x_8}{x_5x_6x_7} + \frac{(x_5+x_6)(x_5x_7+x_6x_7+x_8)}{x_4x_6x_8} + \frac{x_5x_7+x_6x_7+x_8}{x_4x_5x_7} + x_4$$

which is (14). Thus the ray map ρ in (11) has matrix

$$\begin{pmatrix} 0 & -1 & -1 & 1 & 0 & 0 & 0 & 0 \\ -1 & 0 & -1 & 0 & 1 & 0 & 0 & 0 \\ -1 & -1 & 0 & 0 & 0 & 1 & 0 & 0 \\ -1 & 0 & -1 & 0 & 0 & 0 & 1 & 0 \\ 1 & -1 & 0 & 0 & 0 & 0 & 0 & 1 \end{pmatrix} \tag{17}$$

and the weight matrix D for the toric variety Y is

$$\begin{pmatrix} 1 & 0 & 0 & 0 & 1 & 1 & 1 & -1 \\ 0 & 1 & 0 & 1 & 0 & 1 & 0 & 1 \\ 0 & 0 & 1 & 1 & 1 & 0 & 1 & 0 \end{pmatrix} \tag{18}$$

The line bundles here are

$$L = \sum_{j \in S_1} D_j = \mathcal{O}(2,1,1) \qquad\qquad L' = \sum_{j \in S_2} D_j = \mathcal{O}(0,1,1)$$

and our analysis suggests that we should consider a Fano variety X_1 cut out of a toric variety Y_1 with ray map (17) by a section of $L \oplus L'$. Since L' occurs as the toric divisor given by the fourth column of (18), we remove the fourth column and also L', considering instead the toric variety Y_1 obtained as a GIT quotient $\mathbb{C}^7 /\!\!/ (\mathbb{C}^\times)^3$ where the weight matrix for the action is

$$\begin{pmatrix} 1 & 0 & 0 & 1 & 1 & 1 & -1 \\ 0 & 1 & 0 & 0 & 1 & 0 & 1 \\ 0 & 0 & 1 & 1 & 0 & 1 & 0 \end{pmatrix} \tag{19}$$

and the subvariety $X_1 \subset Y_1$ cut out by a section of $L \cong \mathcal{O}(2,1,1)$.

To specify Y_1, we need to choose a stability condition for the GIT quotient $Y_1 = \mathbb{C}^7 /\!\!/ (\mathbb{C}^\times)^3$; equivalently, we need to choose the fan for Y, and the weight matrix (19) only determines the rays of this fan. For this we examine the secondary fan. The secondary fan is the cone spanned by the columns of (19), which we picture by intersecting it with the plane $x + 2y + z = 1$ and projecting to the xy-plane, equipped with the wall-and-chamber decomposition shown in Figure 11. Choosing the stability condition that makes Y_1 into a Fano toric variety, i.e. $-K_{Y_1} = \mathcal{O}(3,3,3)$, which is shown as a hollow circle in Figure 11, results in a non-$\mathbb{Q}$-factorial toric variety. We instead choose the stability condition $-K_{Y_2} - L = \mathcal{O}(1,2,2)$, which lies in the interior of the shaded chamber. This specifies a toric orbifold Y_1, and ensures that the subvariety $X_1 \subset Y_1$ cut out by a general section of L is Fano.

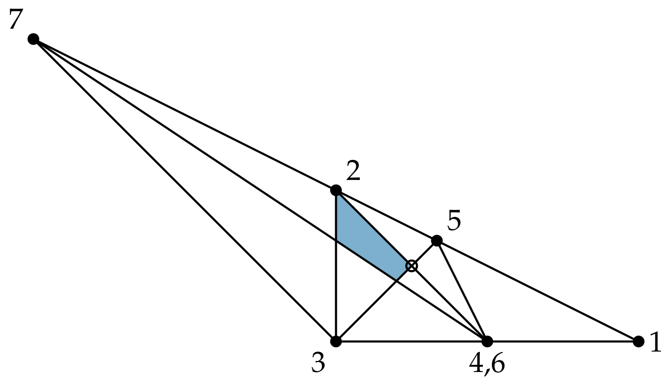

Figure 11. A slice of the secondary fan of Y_1. The shaded region is the stability chamber.

It remains to determine the singularities of a general section of L. Fix Cox co-ordinates $(z_1, z_2, \ldots, z_7)$ on Y_2 compatible with (19). There are precisely twelve maximal charts on Y_1, each of the form $U_{ijk} := \{z_i = z_j = z_k = 1\}$ where the cone $\langle ijk \rangle$ contains the shaded chamber in its strict interior. Only three of them are singular: U_{357}, U_{457} and U_{567}. A general section of L is of the form

$$z_1^3 z_3 z_7 + z_4 z_5 + z_1 z_2 z_4 + z_5 z_6 + z_1^2 z_4 z_7 + z_1 z_3 z_5 + z_1 z_2 z_6 + z_1^2 z_2 z_3 + z_1^2 z_6 z_7$$

where as usual we omit generic coefficients from the equation. We see that:

- The singular locus of Y_1 consists of the origins of the three singular charts and the curve $C = \{z_1 = z_2 = z_3 = 0\}$.
- A general section of L does not pass through the origins of U_{457} and U_{567}, but does pass through the origin of U_{357}. This gives rise to a singularity on X_1 of type $\frac{1}{2}(1,1,1)$: the chart on Y_1 is $\frac{1}{2}(1,1,1,1)_{1246}$ and $L = \mathcal{O}(1)$ here.
- A general section of L meets C in an isolated point of type $\frac{1}{2}(1,1,1)$.

Thus a general section of L is singular in precisely two points, and each is of type $\frac{1}{2}(1,1,1)$.

4.3.2. *The scaffolding of f_2.* This is

$$f_2 = (1+z)y + \frac{(1+z)^2(1+y)}{xyz} + \frac{1+y}{x} + x$$

which gives $c = 2$ and

$$\theta_1(x,y,z) = 1+z$$
$$\theta_2(x,y,z) = 1+y$$

Thus $|S_1| = |S_2| = 2$. Shifting the constant term again, we consider

$$2 + (1+z)y + \frac{(1+z)^2(1+y)}{xyz} + \frac{1+y}{x} + x$$

This gives $|S_0| = 4$, and the weight matrix (8) as

$$\begin{pmatrix} -1 & -2 & 0 & 0 & 1 & 1 & 0 & 0 \\ 0 & -1 & -1 & 0 & 0 & 0 & 1 & 1 \end{pmatrix}$$

In co-ordinates $(x_1, x_2, \ldots, x_8)$ with $x_4 = x$, $x_6 = z$, and $x_8 = y$ we see that f homogenises to

$$2 + \frac{(x_5+x_6)x_8}{x_5x_7} + \frac{(x_5+x_6)^2(x_7+x_8)}{x_4x_5x_6x_8} + \frac{x_7+x_8}{x_4x_7} + x_4$$

which is (14). Thus the ray map ρ in (11) has matrix

$$\begin{pmatrix} 0 & -1 & -1 & 1 & 0 & 0 & 0 & 0 \\ -1 & -1 & 0 & 0 & 1 & 0 & 0 & 0 \\ 0 & -1 & 0 & 0 & 0 & 1 & 0 & 0 \\ -1 & 0 & -1 & 0 & 0 & 0 & 1 & 0 \\ 1 & -1 & 0 & 0 & 0 & 0 & 0 & 1 \end{pmatrix}$$

and the weight matrix D for the toric variety Y is

$$\begin{pmatrix} 1 & 0 & 0 & 0 & 1 & 0 & 1 & -1 \\ 0 & 1 & 0 & 1 & 1 & 1 & 0 & 1 \\ 0 & 0 & 1 & 1 & 0 & 0 & 1 & 0 \end{pmatrix} \tag{20}$$

The line bundles are

$$L = \sum_{j \in S_1} D_j = \mathcal{O}(1,2,0) \qquad\qquad L' = \sum_{j \in S_2} D_j = \mathcal{O}(0,1,1)$$

Once again we remove both the fourth column of (20) and L', and consider the toric variety Y_2 obtained as a GIT quotient $\mathbb{C}^7 /\!\!/ (\mathbb{C}^\times)^3$ where the weight matrix for the action is

$$\begin{pmatrix} 1 & 0 & 0 & 1 & 0 & 1 & -1 \\ 0 & 1 & 0 & 1 & 1 & 0 & 1 \\ 0 & 0 & 1 & 0 & 0 & 1 & 0 \end{pmatrix} \tag{21}$$

and the subvariety $X_2 \subset Y_2$ cut out by a section of $L \cong \mathcal{O}(1,2,0)$.

To specify the stability condition for the GIT quotient $Y_2 = \mathbb{C}^7 /\!\!/ (\mathbb{C}^\times)^3$, we examine the secondary fan. This is the cone spanned by the columns of (21), which we again picture by intersecting it with the plane $x + 2y + z = 1$ and projecting to the xy-plane, equipped with the wall-and-chamber decomposition shown in Figure 12. Choosing the stability condition that makes Y_2 into a Fano toric variety, i.e. $-K_{Y_2} = \mathcal{O}(2,4,2)$, which is shown as a hollow circle in Figure 12, again results in a toric variety that is not $\mathbb{Q}$-factorial. We instead choose the stability condition $-K_{Y_1} - L = \mathcal{O}(1,2,2)$, which lies in the interior of the shaded chamber. This specifies a toric orbifold Y_2, and ensures that the subvariety $X_2 \subset Y_2$ cut out by a general section of L is Fano.

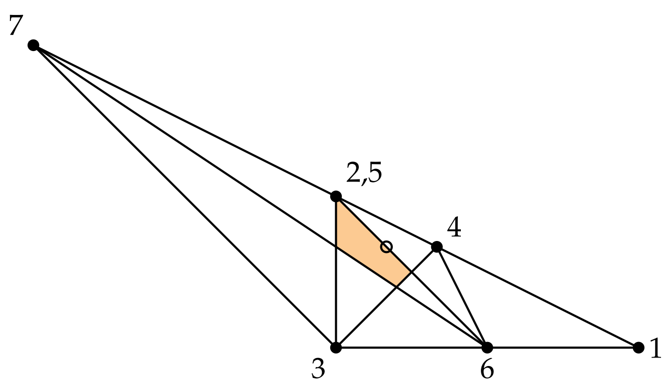

Figure 12. A slice of the secondary fan of Y_2. The shaded region is the stability chamber.

Once again we analyse the singularities of a general section of L, working in Cox co-ordinates $(z_1, z_2, \ldots, z_7)$ compatible with (21). Again there are exactly twelve maximal charts on Y_2, each of the form $U_{ijk} := \{z_i = z_j = z_k = 1\}$ where the cone $\langle ijk \rangle$ contains the shaded chamber in its strict interior. Only two of them are singular: U_{347} and U_{467}. A general section of L is of the form

$$z_1z_5^2 + z_4z_5 + z_1^3z_7^2 + z_1^2z_2z_7 + z_1^2z_5z_7 + z_1z_2^2 + z_1z_4z_7 + z_1z_2z_5 + z_2z_4$$

and hence passes through the origins of both singular charts. This gives rise to two singularities on X_2 of type $\frac{1}{2}(1,1,1)$: the charts on Y_2 are $\frac{1}{2}(1,1,1,1)_{1256}$ and $\frac{1}{2}(1,1,1,1)_{1235}$, and in each chart $L = \mathcal{O}(1)$. Thus again a general section of L is singular in precisely two points, each of type $\frac{1}{2}(1,1,1)$.

The varieties X_1 and X_2 are distinct. To compute the regularised quantum periods of X_1 and X_2, we argue as in [23, Corollary D.5], but using the mirror theorem for toric complete intersections due to J. Wang [68] in place of the Quantum Lefschetz theorem and Givental's mirror theorem for toric manifolds. This yields

$$\widehat{G}_{X_1}(t) = 1 + 4t^2 + 18t^3 + 60t^4 + 600t^5 + 2470t^6 + 18900t^7 + 118300t^8 + 723240t^9 + \cdots$$
$$\widehat{G}_{X_2}(t) = 1 + 6t^2 + 18t^3 + 90t^4 + 780t^5 + 3210t^6 + 28560t^7 + 164010t^8 + 1146600t^9 + \cdots$$

Thus X_1 and X_2 are not deformation equivalent. Note also that, as the singularities of X_1 and X_2 are isolated, they are rigid [66], and therefore we cannot smooth X_1 or X_2 (or X_P) further in their deformation-equivalence classes.

5. Systematic generation of hypersurface examples

One can explore the landscape of Fano manifolds by systematically generating complete intersection models [29], but this approach is much less effective in the $\mathbb{Q}$-Fano (orbifold) setting. That is because, unless the ambient space is a weighted projective space [47], we lack combinatorial criteria to detect whether a complete intersection is quasismooth, and thus checking quasismoothness involves computationally expensive Gröbner basis calculations. It turns out, however, that we can restore the effectiveness of this method in the $\mathbb{Q}$-Fano setting by combining the systematic generation of toric complete intersections with an analysis of their Laurent polynomial mirrors. By restricting attention to those toric complete intersections such that the Givental/Hori–Vafa mirror is a maximally mutable Laurent polynomial, one can sidestep many expensive quasismoothness checks that we expect, in general, will fail. In this section we use this approach to generate $\mathbb{Q}$-Fano threefolds that are hypersurfaces in toric orbifolds. One should regard this as a proof of concept: the methods apply without significant change to complete intersections in higher-dimensional toric varieties as well.

We randomly generated $\mathbb{Q}$-Fano threefolds that occur as toric hypersurfaces, by taking the following steps.

(1) We generated 2×6 integer matrices W and length-2 integer vectors D with small non-negative integer entries. Specifically, we chose entries in W and D uniformly at random from the set $\{0, 1, \ldots, 6\}$.
(2) We discarded (W, D) unless:
   (a) the four-dimensional Fano toric variety Y with weight matrix W was $\mathbb{Q}$-factorial;
   (b) the line bundle $L \to Y$ defined by the weight vector D was nef; and
   (c) $-K_Y - L$ was ample on Y.

   These are combinatorial conditions on the entries of W and L. Condition (2c) here guarantees that the threefold cut out by a general section of L is Fano.
(3) We discarded (W, D) unless:
   (a) D did not occur as a column of W.

(b) the $\mathbb{Q}$-Fano threefold X cut out by a general section of L had a truncated period sequence $c_0, c_1, \ldots, c_N$ such that

$$\gcd\{d : c_d \neq 0\} = 1$$

That is, it did not have the pattern of zeroes characteristic of Fano varieties with Fano index greater than one.

(c) the weight matrix and the divisor satisfied the conditions for the Givental/Hori–Vafa method to give a Laurent polynomial f mirror to X [29, §5].

(d) the Hilbert series of X was present in the database of possible Hilbert series of semistable $\mathbb{Q}$-Fano threefolds [10]. Note that such a Hilbert series uniquely determines a set of singularities, called the basket, such that any $\mathbb{Q}$-Fano threefold with that Hilbert series has singular set equal to the basket [5, 13].

(e) the weight matrix W satisfied certain divisibility conditions that are necessary if the toric variety Y is to contain a quasismooth hypersurface with singular set equal to the basket from (3d).

(4) We discarded (W, D) unless the Laurent polynomial mirror f from (3c) was rigid maximally mutable.

(5) We discarded (W, D) unless the hypersurface X cut out by a randomly chosen section of L was quasismooth with isolated singularities.

From just under 5 000 000 examples after step 1, we found 160 762 examples after step 2, then 7 272 examples after step 3, then 354 examples after step 4, and 333 examples after step 5.

Note that a single $\mathbb{Q}$-Fano threefold can correspond to many different Laurent polynomials. But conjecturally these Laurent polynomials are all related by mutation, and in particular have the same period sequence; indeed we expect that a $\mathbb{Q}$-Fano threefold is uniquely determined by its period sequence. The 333 Laurent polynomials above gave rise to 130 distinct period sequences. Of these, 32 were not among the period sequences of rigid MMLPs with canonical Newton polytope (as pictured in Figure 1(b)), and 15 occurred among the examples constructed using Laurent inversion in [45]. The position of the 130 period sequences in the landscape of $\mathbb{Q}$-Fano threefolds is indicated in Figure 13; see also Figure 1(e) above.

6. Towards a Classification Theorem

If Conjecture 2 holds, along with the surrounding conjectural picture discussed in §1, then the classification of $\mathbb{Q}$-Fano threefolds would follow from understanding:

(1) Given a rigid MMLP, how can we construct the corresponding Fano variety?
(2) How can we find a representative rigid MMLP for every $\mathbb{Q}$-Fano threefold?

Let us make the latter question more precise:

(2′) Given a finite set of deformation-equivalence classes of $\mathbb{Q}$-Fano threefolds, how can we find a representative rigid MMLP for every Fano variety in this set?

One natural way to create the finite sets in (2′) is by bounding the complexity of the singularities allowed [8].

(2″) Given a bound on the complexity of the singularities of a $\mathbb{Q}$-Fano threefold, how can we find a representative rigid MMLP for every Fano variety that satisfies this bound?

6.1. Towards answering question 1.

Laurent inversion is a powerful tool for addressing question 1. But it is clearly not enough, because not every $\mathbb{Q}$-Fano threefold is a toric complete intersection. There has been some progress in constructing $\mathbb{Q}$-Fano threefolds in Pfaffian format from scaffoldings with shapes based on the toric surface dP_7 [45].

Problem A: Generalise Laurent inversion to Fano varieties presented in Pfaffian format.

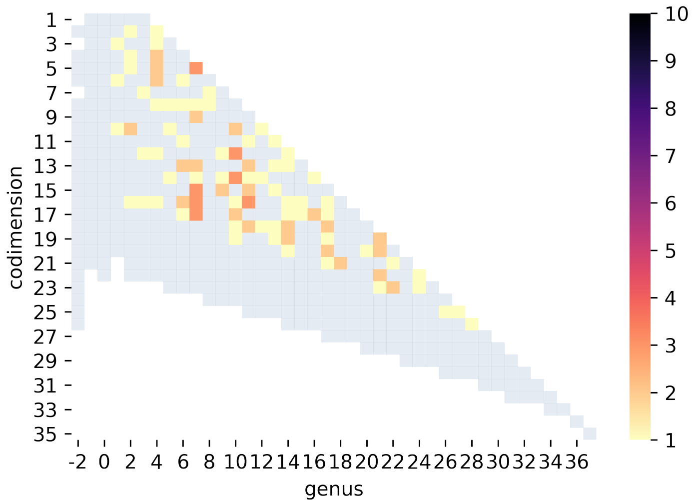

Figure 13. The distribution of Hilbert series for randomly generated $\mathbb{Q}$-Fano quasi-smooth threefold hypersurfaces in $\mathbb{Q}$-factorial toric varieties of Picard rank 2. Hilbert series are recorded as pairs (c, g) where c is the estimated codimension and g is the genus.

Furthermore every smooth Fano threefold is a *quiver flag zero locus*, that is, a zero locus of a section of a homogeneous vector bundle over a GIT quotient of a vector space by a product of general linear groups [23, 48]. Many toric complete intersections are also quiver flag zero loci, and generalising Laurent inversion to quiver flag zero loci would be an important source of new constructions.

Problem B: Generalise Laurent inversion to quiver flag zero loci.

Note that recent work of Webb allows the analysis of quiver flag zero loci that are orbifolds [69]. Kalashnikov has produced 99 rigid MMLPs in four variables that are conjectural mirrors to quiver flag zero loci [49]; this should be an important source of test cases.

An additional challenge is that, as things stand, applying Laurent inversion requires substantial ingenuity, particularly in the construction of scaffoldings. There are many deformation classes of $\mathbb{Q}$-Fano threefolds, far more than it would be practical to construct by hand.

Problem C: Develop effective algorithms to automate Laurent inversion.

In order to construct the classification, and even to explore it at scale, we will need to use Laurent inversion as part of computer algebra calculations.

One of the most effective tools for constructing $\mathbb{Q}$-Fano threefolds in low codimension is Tom and Jerry [15, 16]. Relating this technique to the analysis of rigid MMLPs would potentially be very powerful, in particular because constructing Laurent inversion models in low codimension seems to be difficult.

Problem D: Understand the relationship between Tom and Jerry, or more generally projection and unprojection, and mirror symmetry.

6.2. **Towards answering question 2.** In order to approach question 2, we need to understand how to determine geometric properties of a Fano variety X from a Laurent polynomial f that corresponds to X under mirror symmetry, or from the Newton polytope $P = \operatorname{Newt} f$. In particular, to answer question $2''$, we need to understand how to determine the singularities of X from f or from P. This will have two consequences for our search:

- given a polytope P, it will help us to predict a $\mathbb{Q}$-Fano threefold to which X_P deforms;

- given a basket of singularities $\mathcal{B}$, it will help us to bound the class of polytopes P that we need to analyse in order to find rigid MMLP representatives for all $\mathbb{Q}$-Fano threefolds with that basket.

In both cases the polytope P occurs as the Newton polytope of a rigid MMLP f that corresponds to X.

In two dimensions we have good control over question 2′′, through the notion of *singularity content* [3]. A Fano polygon P determines a collection of singularities $\mathcal{B}$, again called the *basket*, with the property that a general qG partial smoothing of X_P has singularities given by $\mathcal{B}$. The basket $\mathcal{B}$ is given combinatorially as follows. Each edge E of P lies at some lattice height r above the origin, and we subdivide E into a number of line segments of length r, plus at most one line segment of length less than r. Making such a choice for each edge E defines a fan Σ, which gives a crepant partial resolution X_Σ of X_P. The line segments of length equal to their lattice height define T-singularities [57] on X_Σ; the remaining singularities on X_Σ are qG-rigid, and define the basket $\mathcal{B}$. It is not clear *a priori* that the basket $\mathcal{B}$ is independent of choices made, but this turns out to be the case.

As indicated, in two dimensions singularity content plays two roles:

- given a polygon P, it determines the singularities on a orbifold del Pezzo surface to which X_P deforms;
- given a basket of singularities $\mathcal{B}$, it determines the class of polygons that we need to analyse in order to find rigid MMLP representatives for all orbifold del Pezzo surfaces with basket $\mathcal{B}$. This is the class of lattice polygons with singularity content $\mathcal{B}$, under the equivalence relation given by combinatorial mutation [2].

This approach allows us to classify orbifold TG del Pezzo surfaces with a given basket [1,20,21, 33,35,53]. Note that singularity content is defined in terms of the polygon P, rather than than a MMLP f with Newton polygon P. This is consistent with the fact that in two dimensions there is a unique family of maximally mutable Laurent polynomials with a given Newton polygon [28]. As we argue below, to obtain a notion of singularity content in higher dimensions we expect that it will be essential to work with f rather than P.

6.3. **Our pictures of the landscape are unsatisfactory.** Recall that Figure 1(b) was produced by analysing a collection of rigid MMLPs [27]. We believe that this collection of Laurent polynomials contains almost all[5] rigid MMLPs f in three variables such that Newt f is canonical, but that was not so important for the discussion in this paper. Indeed the classes of polytopes that we considered when producing the pictures of the $\mathbb{Q}$-Fano landscape in Figure 1, although natural from the point of view of combinatorics, are not well-adapted to the $\mathbb{Q}$-Fano classification problem. Ideally we would search over a classification of three-dimensional lattice polytopes with fixed singularity content, up to the equivalence given by combinatorial mutation. Fixing the singularity content here would correspond to bounding the complexity of the singularities in the corresponding $\mathbb{Q}$-Fano threefolds. In order to do this, however, we would need an appropriate definition of singularity content for three-dimensional polytopes. This does not yet exist, and so for Figure 1 we had to work with the three-dimensional polytope classifications that are available.

6.4. **Towards singularity content in higher dimensions.** As discussed, singularity content in dimension two is a basket of singularities, which is computed from a polygon P by a crepant resolution procedure. In higher dimensions the situation is more complicated. For example, in dimension three there are global obstructions to smoothability even when all local obstructions

[5] The algorithm that we use has impractically long runtime on several hundred of the 674 688 three-dimensional canonical polytopes.

vanish [61], but this is not the case in two dimensions [1]. Furthermore, in three dimensions X_P can admit many qG-generizations that are not deformation equivalent; this is not the case in two dimensions. Thus any notion of singularity content in higher dimensions must be richer than just a basket of singularities. But nonetheless there are hints that a similar crepant partial resolution procedure might produce the basket for X, together with some extra structure (a triangulation), from its Laurent polynomial mirror f. For example, consider the three-dimensional canonical polytope P shown in Figure 14. This supports two distinct rigid MMLPs

$$f_1 = x^4y^2z^3 + 2x^2yz^2 + 3x + y + z + \frac{2}{xyz} + \frac{3}{x^2y^2z^3} + \frac{1}{x^5y^4z^6}$$
$$f_2 = x^4y^2z^3 + 2x^2yz^2 + 3x + y + z + \frac{3}{xyz} + \frac{3}{x^2y^2z^3} + \frac{1}{x^5y^4z^6}$$

which differ only in the coefficient of $x^{-1}y^{-1}z^{-1}$. The period sequences for f_1 and f_2 are distinct, so we expect that there are two deformation families of $\mathbb{Q}$-Fano threefold that qG-degenerate to X_P. One of these families can be constructed by applying Laurent inversion to the scaffolding shown in Figure 15, which is mutation-equivalent to f_2; we do not know how to construct the other deformation family.

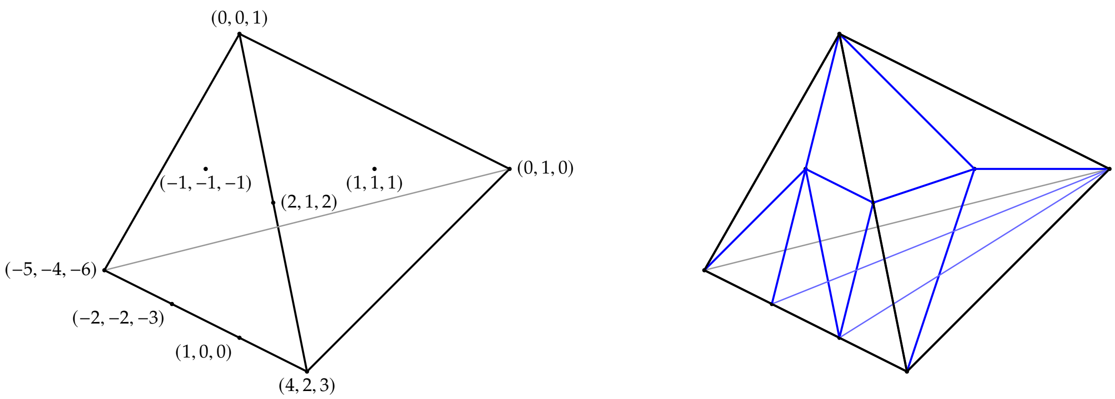

Figure 14. A boundary triangulation of the three-dimensional canonical polytope with ID 547307 in the Graded Ring Database [11].

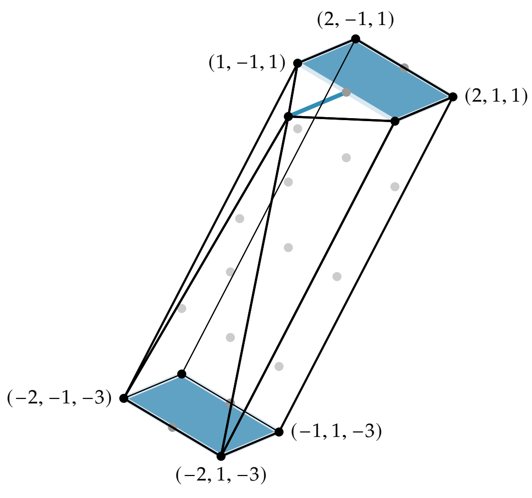

Figure 15. A scaffolding of a Laurent polynomial that is mutation-equivalent to f_2.

Consider in addition a triangulation of the boundary of P as shown in Figure 14, and form a fan by taking cones over each triangle in the triangulation. The left-hand front facet gives rise to six smooth cones, and the right-hand front facet gives to four smooth cones. The back facet gives a singularity of type $\frac{1}{5}(1,1,4)$, and the bottom facet gives three singularities of type $\frac{1}{3}(1,1,2)$; these singularities are terminal and qG-rigid. This suggests a basket

$$\mathcal{B} = \left\{3 \times \tfrac{1}{3}(1,1,2), \tfrac{1}{5}(1,1,4)\right\}$$

which agrees with the basket calculated from the Ehrhart series of P^*, that is, with the basket of the possible $\mathbb{Q}$-Fano Hilbert series with ID 29915 in the Graded Ring Database[6]. In this particular example any triangulation such that the faces are divided into empty triangles will give the same result: the front two faces are both at lattice height 1 above the origin, and so any triangulation of them will give rise to a total of 10 smooth cones. There is no choice for the triangulation of the other two faces, at least if we insist on the triangles on the bottom face being empty.

For a second example, consider the Laurent polynomial

$$f = \frac{(x^2 + 2x + yz^3 + 3yz^2 + 3yz + y + 1)^2}{xyz} - 12$$

which is mirror to the smooth Fano 3-fold V_6. (It is easy to check that f is mutation-equivalent to the Laurent polynomial mirror to V_6 given in [23, Appendix A].) The Newton polytope Q of f is pictured in Figure 16. Since the Fano variety V_6 is smooth, we expect that Q should have empty basket; indeed the Ehrhart series of Q^*, which is the possible $\mathbb{Q}$-Fano Hilbert series with ID 24076 in the Graded Ring Database, has empty basket. As before, let us consider a

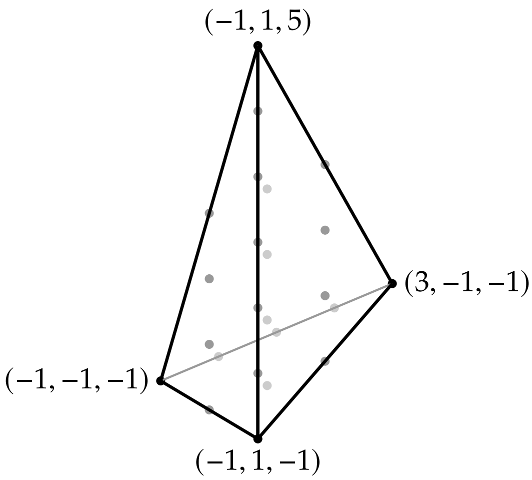

Figure 16. The Newton polytope Q of a Laurent polynomial mirror to V_6.

triangulation of the boundary of Q, and form a fan by taking cones over each triangle in the triangulation. Each face of Q other than the back face has lattice height 1 above the origin, and the back face has lattice height 2. So let us insist that our triangulation contains only empty

[6]Recall that we expect that, if a Fano variety X corresponds under mirror symmetry to a Laurent polynomial f, then there is a qG-degeneration from X to X_f. This implies that the Hilbert series of X coincides with the Hilbert series of X_f, and hence with the Ehrhart series of the dual polytope P^* where $P = \mathrm{Newt}(f)$. Thus the Hilbert series of X is determined by the Newton polytope P of f. Furthermore the singularities of a $\mathbb{Q}$-Fano threefold X are uniquely determined by its Hilbert series, and hence by P. The fact that the singularities of a $\mathbb{Q}$-Fano threefold are determined by its Hilbert series seems to be a combinatorial accident: it is established by looking case by case through the Graded Ring Database [13], and lacks a geometric proof. We see no reason for the corresponding statement to be true for higher-dimension $\mathbb{Q}$-Fano varieties. Thus it is likely that, in dimension four and higher, even the basket $\mathcal{B}$ of a $\mathbb{Q}$-Fano qG-generization X of X_f will depend on the rigid MMLP f that corresponds to X, and not just on the Newton polytope of f.

triangles on the front faces and bottom face; these empty triangles will give rise to smooth cones in the fan. For the back face, let us take the triangulation shown in Figure 17. Note that

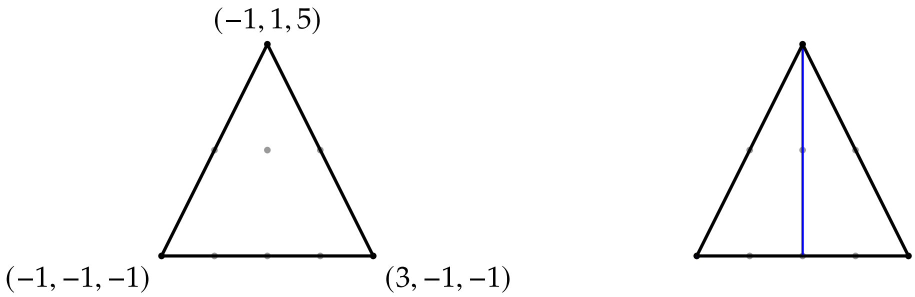

Figure 17. A triangulation of the back facet of Q.

the height of the facet is 2, and that both triangles shown are 2-fold dilations of a standard two-dimensional lattice simplex; note also that all vertices in the triangulation are primitive. This suggests, by analogy with the construction of singularity content in two dimensions, that the singularities that correspond to these cones should be qG-smoothable – that is, we expect these cones to give rise to three-dimensional T-singularities. This would give empty basket for Q, in agreement with the discussion above.

One challenge in passing from this discussion to a satisfactory definition of singularity content in three dimensions is that in general there are many different triangulations of the boundary of a three-dimensional polytope $Q = \operatorname{Newt} f$, and it is not clear (at least to us) which such triangulations should be admissible. We expect that the admissible triangulations will be determined by set S_f of mutations that f permits; this was defined just before Proposition 8. In particular the admissible triangulations will depend on f and not just on the underlying polytope Q. One can see hints of this phenomenon in the work of Corti–Hacking–Petracci on smoothing Gorenstein toric Fano varieties: see [24]. It is likely that singularity content in higher dimensions will closely resemble the Corti–Filip–Petracci notion of zero-mutable Laurent polynomials [31].

Problem E: Give a combinatorial definition of singularity content in all dimensions.

Whatever the definition is, in a fully satisfactory theory there should be a bijection between:

- the data defining the singularity content of rigid MMLPs f with Newton polytope P;
- the set of mutation-equivalence classes of such f;
- the smoothing components of the qG-deformation space of X_P.

This is the picture that holds in two dimensions [1,28], and that we expect to generalise.

Acknowledgments. The research presented here has been guided in a fundamental way by ideas of and joint work with Alessio Corti. It forms part of a broader program, initiated by Corti and Vasily Golyshev, to discover and understand the classification of Fano varieties using mirror symmetry. We thank Corti, Sergey Galkin, Golyshev, Andrea Petracci, and Thomas Prince for many useful conversations. In particular, Conjecture 2 arose from conversations with Corti and Golyshev at the workshop *Motivic Structures on Quantum Cohomology and Pencils of CY Motives* at the Max Planck Institute for Mathematics, Bonn in September 2014.

The computations that underlie this work were performed using the Imperial College High Performance Computing Service and the compute cluster at the Department of Mathematics, Imperial College London. We thank Andy Thomas and Matt Harvey for invaluable technical assistance. TC is supported by ERC Consolidator Grant 682603 and EPSRC Programme Grant EP/N03189X/1. LH is supported by Leverhulme grant RPG-2021-149 and Projet Étoiles montantes Région Pays de la Loire. AK is supported by EPSRC Fellowship EP/N022513/1.

References

[1] Mohammad Akhtar, Tom Coates, Alessio Corti, Liana Heuberger, Alexander M. Kasprzyk, Alessandro Oneto, Andrea Petracci, Thomas Prince, and Ketil Tveiten. Mirror symmetry and the classification of orbifold del Pezzo surfaces. *Proc. Amer. Math. Soc.*, 144(2):513–527, 2016. doi:10.1090/proc/12876.

[2] Mohammad Akhtar, Tom Coates, Sergey Galkin, and Alexander M. Kasprzyk. Minkowski polynomials and mutations. *SIGMA Symmetry Integrability Geom. Methods Appl.*, 8:Paper 094, 17, 2012. doi:10.3842/SIGMA.2012.094.

[3] Mohammad Akhtar and Alexander M. Kasprzyk. Singularity content. arXiv:1401.5458 [math.CO], 2016.

[4] Selma Altınok. *Graded Rings Corresponding to Polarised K3 Surfaces and $\mathbb{Q}$-Fano 3-folds*. PhD thesis, University of Warwick, 1998.

[5] Selma Altinok, Gavin Brown, and Miles Reid. Fano 3-folds, K3 surfaces and graded rings. In *Topology and geometry: commemorating SISTAG*, volume 314 of *Contemp. Math.*, pages 25–53. Amer. Math. Soc., Providence, RI, 2002.

[6] Hülya Argüz and Mark Gross. The higher-dimensional tropical vertex. *Geom. Topol.*, 26(5):2135–2235, 2022. doi:10.2140/gt.2022.26.2135.

[7] Gabriele Balletti and Alexander M. Kasprzyk. Three-dimensional lattice polytopes with two interior lattice points. arXiv:1612.08918 [math.CO], 2016.

[8] Caucher Birkar. Singularities of linear systems and boundedness of Fano varieties. *Ann. of Math. (2)*, 193(2):347–405, 2021. doi:10.4007/annals.2021.193.2.1.

[9] Caucher Birkar, Paolo Cascini, Christopher D. Hacon, and James McKernan. Existence of minimal models for varieties of log general type. *J. Amer. Math. Soc.*, 23(2):405–468, 2010. doi:10.1090/S0894-0347-09-00649-3.

[10] Gavin Brown and Alexander M. Kasprzyk. The Graded Ring Database. Database of possible Hilbert series of $\mathbb{Q}$-factorial terminal Fano 3-folds, online. `http://grdb.co.uk/forms/fano3`.

[11] Gavin Brown and Alexander M. Kasprzyk. The Graded Ring Database. Database of toric canonical 3-folds, online. `http://grdb.co.uk/forms/toricf3c`.

[12] Gavin Brown and Alexander M. Kasprzyk. The Fano 3-fold database. *Zenodo*, doi:10.5281/zenodo.5820338, 2022.

[13] Gavin Brown and Alexander M. Kasprzyk. Kawamata boundedness for Fano threefolds and the Graded Ring Database. arXiv:2201.07178 [math.AG], 2022.

[14] Gavin Brown, Alexander M. Kasprzyk, and Muhammad Imran Qureshi. Fano 3-folds in $\mathbb{P}^2 \times \mathbb{P}^2$ format, Tom and Jerry. *Eur. J. Math.*, 4(1):51–72, 2018. doi:10.1007/s40879-017-0200-2.

[15] Gavin Brown, Michael Kerber, and Miles Reid. Fano 3-folds in codimension 4, Tom and Jerry. Part I. *Compos. Math.*, 148(4):1171–1194, 2012. doi:10.1112/S0010437X11007226.

[16] Gavin Brown, Miles Reid, and Jan Stevens. Tutorial on Tom and Jerry: the two smoothings of the anticanonical cone over $\mathbb{P}(1,2,3)$. *EMS Surv. Math. Sci.*, 8(1-2):25–38, 2021. doi:10.4171/emss/43.

[17] Gavin Brown and Kaori Suzuki. Computing certain Fano 3-folds. *Japan J. Indust. Appl. Math.*, 24(3):241–250, 2007.

[18] Gavin Brown and Kaori Suzuki. Fano 3-folds with divisible anticanonical class. *Manuscripta Math.*, 123(1):37–51, 2007. doi:10.1007/s00229-007-0082-6.

[19] Frédéric Campana and Hubert Flenner. Projective threefolds containing a smooth rational surface with ample normal bundle. *J. Reine Angew. Math.*, 440:77–98, 1993.

[20] Daniel Cavey and Edwin Kutas. Classification of minimal polygons with specified singularity content. In *Interactions with lattice polytopes*, volume 386 of *Springer Proc. Math. Stat.*, pages 115–134. Springer, Cham, 2022. doi:10.1007/978-3-030-98327-7_5.

[21] Daniel Cavey and Thomas Prince. Del Pezzo surfaces with a single $1/k(1,1)$ singularity. *J. Math. Soc. Japan*, 72(2):465–505, 2020. doi:10.2969/jmsj/79337933.

[22] Tom Coates, Alessio Corti, Sergey Galkin, Vasily Golyshev, and Alexander M. Kasprzyk. Mirror symmetry and Fano manifolds. In *European Congress of Mathematics*, pages 285–300. Eur. Math. Soc., Zürich, 2013.

[23] Tom Coates, Alessio Corti, Sergey Galkin, and Alexander M. Kasprzyk. Quantum periods for 3-dimensional Fano manifolds. *Geom. Topol.*, 20(1):103–256, 2016. doi:10.2140/gt.2016.20.103.

[24] Tom Coates, Alessio Corti, and Genival da Silva. On the topology of Fano smoothings. In *Interactions with Lattice Polytopes*, volume 386 of *Proceedings in Mathematics & Statistics*, pages 135–156. Springer, 2022. doi:10.1007/978-3-030-98327-7_6.

[25] Tom Coates, Sergey Galkin, Alexander M. Kasprzyk, and Andrew Strangeway. Quantum periods for certain four-dimensional Fano manifolds. *Exp. Math.*, 29(2):183–221, 2020. doi:10.1080/10586458.2018.1448018.

[26] Tom Coates, Alexander M. Kasprzyk, and Giuseppe Pitton. Computing maximally mutable Laurent polynomials. In preparation.

[27] Tom Coates, Alexander M. Kasprzyk, and Giuseppe Pitton. Certain rigid maximally mutable Laurent polynomials in three variables. *Zenodo*, doi:10.5281/zenodo.6636221, 2022.

[28] Tom Coates, Alexander M. Kasprzyk, Giuseppe Pitton, and Ketil Tveiten. Maximally mutable Laurent polynomials. *Proc. of the Royal Society A.*, 477(2254):Paper No. 20210584, 21, 2021. doi:10.1098/rspa.2021.0584.

[29] Tom Coates, Alexander M. Kasprzyk, and Thomas Prince. Four-dimensional Fano toric complete intersections. *Proc. of the Royal Society A.*, 471(2175):Paper No. 20140704, 14, 2015. doi:10.1098/rspa.2014.0704.

[30] Tom Coates, Alexander M. Kasprzyk, and Thomas Prince. Laurent inversion. *Pure Appl. Math. Q.*, 15(4):1135–1179, 2019. doi:10.4310/pamq.2019.v15.n4.a5.

[31] Alessio Corti, Matej Filip, and Andrea Petracci. Mirror symmetry and smoothing Gorenstein toric affine 3-folds. In *Facets of algebraic geometry. Vol. I*, volume 472 of *London Math. Soc. Lecture Note Ser.*, pages 132–163. Cambridge Univ. Press, Cambridge, 2022.

[32] Alessio Corti, Paul Hacking, and Andrea Petracci. Smoothing Gorenstein toric Fano 3-folds. arXiv:2412.06500 [math.AG], 2024.

[33] Alessio Corti and Liana Heuberger. Del Pezzo surfaces with $\frac{1}{3}(1,1)$ points. *Manuscripta Math.*, 153(1-2):71–118, 2017. doi:10.1007/s00229-016-0870-y.

[34] Stephen Coughlan and Tom Ducat. Constructing Fano 3-folds from cluster varieties of rank 2. *Compos. Math.*, 156(9):1873–1914, 2020. doi:10.1112/s0010437x20007368.

[35] Alice Cuzzucoli. *On the classification of orbifold del Pezzo surfaces*. PhD thesis, University of Warwick, 2020. http://webcat.warwick.ac.uk/record=b3467781~S15.

[36] Charles F. Doran and Andrew Harder. Toric degenerations and Laurent polynomials related to Givental's Landau–Ginzburg models. *Canad. J. Math.*, 68(4):784–815, 2016. doi:10.4153/CJM-2015-049-2.

[37] Tom Ducat. Constructing $\mathbb{Q}$-Fano 3-folds à la Prokhorov & Reid. *Bull. Lond. Math. Soc.*, 50(3):420–434, 2018. doi:10.1112/blms.12150.

[38] Alexander Givental. A mirror theorem for toric complete intersections. In *Topological field theory, primitive forms and related topics (Kyoto, 1996)*, volume 160 of *Progr. Math.*, pages 141–175. Birkhäuser Boston, Boston, MA, 1998.

[39] Mark Gross, Paul Hacking, and Bernd Siebert. Theta functions on varieties with effective anti-canonical class. *Mem. Amer. Math. Soc.*, 278(1367):xii+103, 2022. doi:10.1090/memo/1367.

[40] Mark Gross and Bernd Siebert. Affine manifolds, log structures, and mirror symmetry. *Turkish J. Math.*, 27(1):33–60, 2003.

[41] Mark Gross and Bernd Siebert. Mirror symmetry via logarithmic degeneration data. I. *J. Differential Geom.*, 72(2):169–338, 2006.

[42] Mark Gross and Bernd Siebert. Mirror symmetry via logarithmic degeneration data, II. *J. Algebraic Geom.*, 19(4):679–780, 2010. doi:10.1090/S1056-3911-2010-00555-3.

[43] Mark Gross and Bernd Siebert. Logarithmic Gromov-Witten invariants. *J. Amer. Math. Soc.*, 26(2):451–510, 2013. doi:10.1090/S0894-0347-2012-00757-7.

[44] Christopher D. Hacon and James McKernan. Existence of minimal models for varieties of log general type. II. *J. Amer. Math. Soc.*, 23(2):469–490, 2010. doi:10.1090/S0894-0347-09-00651-1.

[45] Liana Heuberger. $\mathbb{Q}$-Fano threefolds and Laurent inversion. *Nagoya Math. J.*, pages 1–47, 2025. Published online. doi:10.1017/nmj.2024.28.

[46] Kentaro Hori and Cumrun Vafa. Mirror symmetry. arXiv:hep-th/0002222, 2000.

[47] Anthony R. Iano-Fletcher. Working with weighted complete intersections. In *Explicit birational geometry of 3-folds*, volume 281 of *London Math. Soc. Lecture Note Ser.*, pages 101–173. Cambridge Univ. Press, Cambridge, 2000.

[48] Elana Kalashnikov. Four-dimensional Fano quiver flag zero loci. *Proc. of the Royal Society A.*, 475(2225):20180791, 23, 2019. doi:10.1098/rspa.2018.0791.

[49] Elana Kalashnikov. Laurent polynomial mirrors for quiver flag zero loci. *Adv. Math.*, 445:Paper No. 109656, 61, 2024. doi:10.1016/j.aim.2024.109656.

[50] Alexander M. Kasprzyk. Toric Fano three-folds with terminal singularities. *Tohoku Math. J. (2)*, 58(1):101–121, 2006. doi:10.2748/tmj/1145390208.

[51] Alexander M. Kasprzyk. Canonical toric Fano threefolds. *Canad. J. Math.*, 62(6):1293–1309, 2010. doi:10.4153/CJM-2010-070-3.

[52] Alexander M. Kasprzyk. The classification of toric canonical Fano 3-folds. *Zenodo*, doi:10.5281/zenodo.5866330, 2010.

[53] Alexander M. Kasprzyk, Benjamin Nill, and Thomas Prince. Minimality and mutation-equivalence of polygons. *Forum Math. Sigma*, 5:Paper No. e18, 48, 2017. doi:10.1017/fms.2017.10.

[54] Kazuya Kato. Logarithmic structures of Fontaine-Illusie. In *Algebraic analysis, geometry, and number theory (Baltimore, MD, 1988)*, pages 191–224. Johns Hopkins Univ. Press, Baltimore, MD, 1989.

[55] János Kollár. Minimal models of algebraic threefolds: Mori's program. Number 177-178, pages Exp. No. 712, 303–326. 1989. Séminaire Bourbaki, Vol. 1988/89.

[56] János Kollár, Yoichi Miyaoka, Shigefumi Mori, and Hiromichi Takagi. Boundedness of canonical **Q**-Fano 3-folds. *Proc. Japan Acad. Ser. A Math. Sci.*, 76(5):73–77, 2000.

[57] János Kollár and Nicholas I. Shepherd-Barron. Threefolds and deformations of surface singularities. *Invent. Math.*, 91(2):299–338, 1988. doi:10.1007/BF01389370.

[58] Shigefumi Mori. Threefolds whose canonical bundles are not numerically effective. *Ann. of Math. (2)*, 116(1):133–176, 1982. doi:10.2307/2007050.

[59] Shigefumi Mori. Flip theorem and the existence of minimal models for 3-folds. *J. Amer. Math. Soc.*, 1(1):117–253, 1988. doi:10.2307/1990969.

[60] Stavros Argyrios Papadakis and Miles Reid. Kustin-Miller unprojection without complexes. *J. Algebraic Geom.*, 13(3):563–577, 2004. doi:10.1090/S1056-3911-04-00343-1.

[61] Andrea Petracci. Some examples of non-smoothable Gorenstein Fano toric threefolds. *Math. Z.*, 295(1-2):751–760, 2020. doi:10.1007/s00209-019-02369-8.

[62] Thomas Prince. Mutation equivalence of toric Landau-Ginzburg models. arXiv:2006.01477 [math.AG], 2020.

[63] Yuri Prokhorov and Miles Reid. On ℚ-Fano 3-folds of Fano index 2. In *Minimal models and extremal rays (Kyoto, 2011)*, volume 70 of *Adv. Stud. Pure Math.*, pages 397–420. Math. Soc. Japan, [Tokyo], 2016. doi:10.2969/aspm/07010397.

[64] Takeshi Sano. On classifications of non-Gorenstein **Q**-Fano 3-folds of Fano index 1. *J. Math. Soc. Japan*, 47(2):369–380, 1995. doi:10.2969/jmsj/04720369.

[65] Takeshi Sano. Classification of non-Gorenstein **Q**-Fano d-folds of Fano index greater than $d-2$. *Nagoya Math. J.*, 142:133–143, 1996. doi:10.1017/S0027763000005663.

[66] Michael Schlessinger. Functors of Artin rings. *Trans. Amer. Math. Soc.*, 130:208–222, 1968. doi:10.2307/1994967.

[67] Hiromichi Takagi. On classification of ℚ-Fano 3-folds of Gorenstein index 2. I, II. *Nagoya Math. J.*, 167:117–155, 157–216, 2002. doi:10.1017/S0027763000025460.

[68] Jun Wang. A mirror theorem for Gromov–Witten theory without convexity. *Forum Math. Sigma*, 13:Paper No. e72, 2025. doi:10.1017/fms.2025.34.

[69] Rachel Webb. Abelianization and quantum Lefschetz for orbifold quasimap I-functions. *Adv. Math.*, 439:Paper No. 109489, 59, 2024. doi:10.1016/j.aim.2024.109489.

Department of Mathematics, Imperial College London, 180 Queen's Gate, London, UK
Email address: `t.coates@imperial.ac.uk`

Institut de Mathématiques de Marseille (I2M), 3 Place Victor Hugo, 13331 Marseille cedex 3, France
Email address: `liana.heuberger@univ-amu.fr`

School of Mathematical Sciences, University of Nottingham, Nottingham, UK
Email address: `a.m.kasprzyk@nottingham.ac.uk`